Universidad de Valladolid

ESCUELA DE INGENIERÍAS INDUSTRIALES

UNIVERSIDAD DE VALLADOLID

ESCUELA DE INGENIERIAS INDUSTRIALES

Máster en Ingenieria ambiental

ENHANCING DIRECT INTERSPECIES ELECTRON TRANSFER THROUGH CO- IMMOBILIZATION OF ANAEROBIC MICROBES USING A CONDUCTIVE SPONGE

Álvarez de la Torre Adrián

Raúl Muñoz Torre

Soka university

Valladolid, Septiembre 2024.

TFM REALIZADO EN PROGRAMA DE INTERCAMBIO

TÍTULO: Enhancing direct interspecies electron transfer through co- immobilization of anaerobic microbes using a conductive sponge
ALUMNO: Adrián Álvarez de la Torre
FECHA: 12-07-2024
CENTRO: Soka university
UNIVERSIDAD: Soka university
TUTOR: Juniichi Ida

Resumen

Anaerobic Digestion (AD) is a biological process which can produce methane by treating organic waste. Recently, it has been discovered that adding conductive materials (CMs) to the AD process can induce direct interspecies electron transfer (DIET) between exoelectrogenic and electrotrophic bacteria, enhancing the efficiency of methane production. However, in a continuous operation, washout of CM remains a challenge today especially in upflow anaerobic sludge blanket (UASB) reactors. Thereby, in this study, enhancing DIET by co-immobilizing anaerobic microbes in a nickel conductive sponge synthesized via the electroless plating method to improve AD performance was attempted. Nickel-plated Melamine sponge (MS) and Polyurethane sponge (PS) were evaluated to select a suitable sponge for the AD process. Despite higher biomass attachment on MS compared to PS, nickel peeling was observed, leading to the selection of PS instead. In the AD experiment, Ni plated PS achieved a higher TOC removal rate, suggesting enhanced organic matter removal and process stability through DIET.

Keywords: Direct Interspecies Electron Transfer, Conductive Material, Nickel Plated Sponge, Anaerobic Digestion

Table of Contents

Table of Contents

Chapter 1: Introduction

1.1 Organic waste generation

Since the earliest days of civilization, organic waste generation has been an inescapable aspect of human existence, presenting both challenges and opportunities (Kurita et al., 2016). The production of organic waste is rapidly increasing worldwide, driven by the growth of the human population and their activities, encompassing household and industrial sources as well (Wärff C.,2020) (Liu et al., 2021). When these wastes are discharged into the environment without proper treatment, they release a high Chemical Oxygen Demand (COD), which serves as an indicator for organic contamination and can result in greenhouse gas emission, water pollution and eutrophication among other environmental issues (Shete & Shinkar, 2013). Therefore, it is essential to implement appropriate wastewater treatment methods to prevent the release of organic waste into the environment.

1.2 Anaerobic digestion process in treating organic waste

One of the most efficient and sustainable methods for treating organic wastes is Anaerobic Digestion (AD) (Rajeshwari et al., 2000). This process is carried out by microorganisms in the absence of oxygen, which can convert organic matter into value-added products, such as biogas and fertilizing materials (Angelidaki et al., 2003). The AD process consists of four distinct stages driven by the metabolic reactions of different microbes (Figure 1) (Baek et al., 2018). First in the hydrolysis process, hydrolysis bacteria break down complex organic wastes into reduced organic compounds, including amino acids, alcohol, sugars and fatty acids, which are subsequently transformed to volatile fatty acids (VFAs) during the acidogenesis process. Following the acetogenesis process, acetogenic bacteria play a crucial role by converting VFAs into acetic acid while simultaneously producing hydrogen and carbon dioxide as a final product of their

metabolism. Then the methanogens will convert acetate or carbon dioxide and electrons in the form of hydrogen to produce methane (Park et al., 2018). This process not only treats organic waste but also generates methane gas, which can be used as an energy source, thereby reducing the costs of the treatment process. Nevertheless, it is well known that anaerobic microbes, especially methanogens, are very sensitive to environmental conditions such as pH, Organic Loading Rate (OLR) and temperature, which makes it necessary to carefully control these parameters. Besides, the syntrophic association between Acetogenic bacteria and Methanogenic archaeal is known as a bottleneck due to the slow electron transfer rate by hydrogen (Figure 2-A) (Baek et al., 2018). Thus, when a high OLR is supplied, the process would face an increase of hydrogen pressure which could inhibit the acetogenic reaction (He et al., 2022). This will further lead to accumulation of volatile fatty acids (VFAs) and then subsequently dropping the pH in the reactor. It should be noted that AD process has been reported to obtain maximum biogas yield when the pH range is between 6.5-7.5, and methanogens will be inhibited when pH drops below 6.5 leading to process failure (C. Liu et al., 2008).

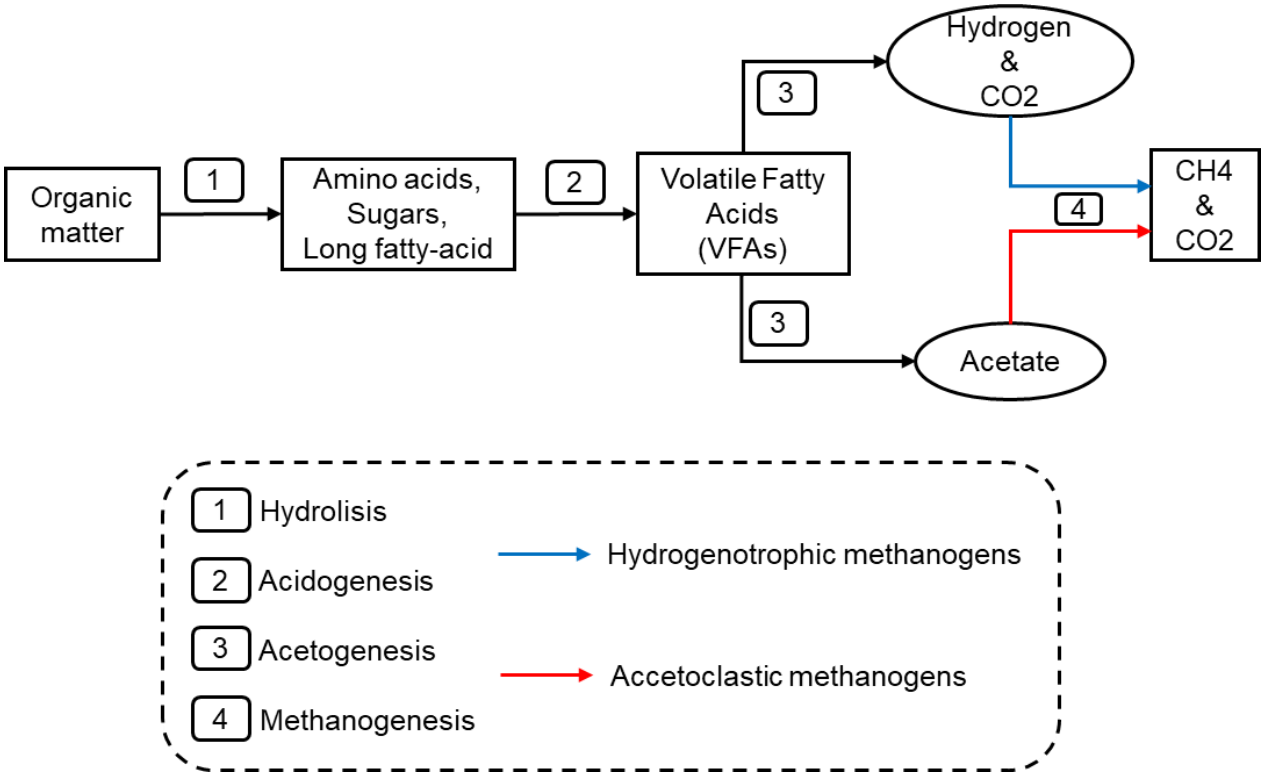

Figure 1. Anaerobic digestion process of degrading organic matter to methane and carbon dioxide

1.3 Direct Interspecies Electron Transfer (DIET) mechanism in Anaerobic Digestion

Recently, numerous studies have shown that the Direct Interspecies Electron Transfer (DIET) mechanism could significantly overcome this "bottleneck". In the process of DIET, acetogenic bacteria can transfer electrons directly to methanogens without requiring hydrogen production for electron exchange (Xiao et al., 2021) (Figure 2A). Since electron transfer rate was demonstrated to be faster than the hydrogen transfer rate (Storck et al., 2015) AD via DIET could perform more efficiently even under a high OLR conditions (Wang et al., 2021). Nevertheless, it should be noted that not all the anaerobic microbes can induct the DIET mechanism but only exoelectrogenic bacteria possess this capability (Yan et al., 2023). To date, the *Geobacter* species which is one of the most known exoelectrogenic bacteria could participate in the DIET mechanism by transferring electron using its biological conductive nanowire (Lovley & Walker, 2019). Other than using its nanowire, there are also different electron transfer mechanisms have been confirmed such as using the microbes' membrane-bound electron transport proteins, or the addition of non-biological conductive materials, which will be detailed below as follows.

1.3.1 DIET via biological conductive nanowires

Figure 2-B depicts the DIET process via biological conductive nanowires, which is one of the extracellular electron exchange mechanisms involving electrically conductive filaments. The nanowires are peptide/protein conductive filaments that play a crucial role in extracellular electron transfer in several organisms, with one of them from the *Geobacter sp.* (Sure et al., 2016). These filaments have been studied in detail to understand their function and significance in the microbial electron transfer process. The nanowires efficiently transfer electrons between the cytochromes of electron-donating and electron-accepting organisms (Malvankar & Lovley, 2014). In the AD field,

Geobacter sp. have been found to transfer electrons to methanogens using nanowires, as long as both microorganisms remain in contact. This interaction enables methanogens to directly receive the electron from the nanowire and convert these compounds into methane (Yan et al., 2023b) (Mei et al., 2018).

1.3.2 DIET via biological Electrical Connections at the Outer Cell Surface

Figure 2-C shows the DIET process via biological Electrical Connections at the Outer Cell Surface. Instead of using the conductive nanowires as interspecies electrical connectors, the DIET mechanism can also be prevailed when cells are tightly connected to each other by transferring electrons through its outer surface's membrane. This phenomenon was observed in cocultures of *Prosthecochloris aestuarii* and *Geobacter sulfurreducens*, where *P. aestuarii*, an anaerobic phototrophic, directly accepts electrons to support photosynthesis (Ha et al., 2017). Unlike other *Geobacter* cocultures, *P. aestuarii* and *G. sulfurreducens* form intimate associations without large aggregates. Deletion of *G. sulfurreducens* genes essential for extracellular electron transfer inhibits co culture growth, indicating DIET. Although pili positive for heme are present, *G. sulfurreducens* can perform cytochrome-dependent electron transfer without e-pili. The multiheme outer-surface cytochrome OmcZ is crucial for effective electron transfer in these cocultures. Additionally, studies have shown that membrane fusions between *P. aestuarii* and *G. sulfurreducens* microbes may facilitate DIET (Lovley, 2017b). However, it should be noted that this process has not been reported in the anaerobic digestion processes, indicating that it may not be a common mechanism in AD.

1.3.3 DIET via non-biological conductive material

Figure 2-D depicts the DIET process via non-biological conductive material. Besides the outer cell surface or the conductive nanowire connections, addition of non-biological conductive materials (CMs) also induce DIET between syntrophic and

methanogenic consortia (Joicy et al., 2022). Various conductive materials, such as carbon-based (Granular Activated Carbon (GAC), Powdered Activated Carbon (PAC), biochar, graphite), iron-based (Magnetite) or even conductive polymers (polyaniline nanorods), have been employed to induce DIET in methane production (Gahlot et al., 2021). CMs exhibit diverse characteristics, such as its large specific surface area, surface-functional groups, porous structure or high conductivity. Some carbon-based materials, for instance biochar or GAC can even absorb inhibitor elements to the AD process performance (Kong & Zhang, 2023) On the other hand, among the different metallic conductive materials, iron oxide-based minerals such as hematite or magnetite can enhance the methanogenesis in terms of lag time and production (Kato et al., 2012) (Kato et al., 2011). Therefore, using different CM can influence the microbial attachment performance and, subsequently, enhance the methane production rate performance. Additionally, since most of the CMs show a higher conductivity than nanowire, which is usually from 2-20 μS/cm (F. Liu et al., 2012), it is expected that the electrons could transfer faster when using a CM instead and save cell energy since no additional energy is needed for the synthesis of biological conductive nanowire (Wu et al., 2020) (Zhao et al., 2016). Furthermore, for exoelectrogenic bacteria that do not naturally produce biological conductive nanowires such as microbes with biological electrical connections at the outer cell surface, the introduction of CMs to induce the DIET mechanism could expand the range of exoelectrogenic bacteria capable of facilitating DIET (B. Guo et al., 2020).

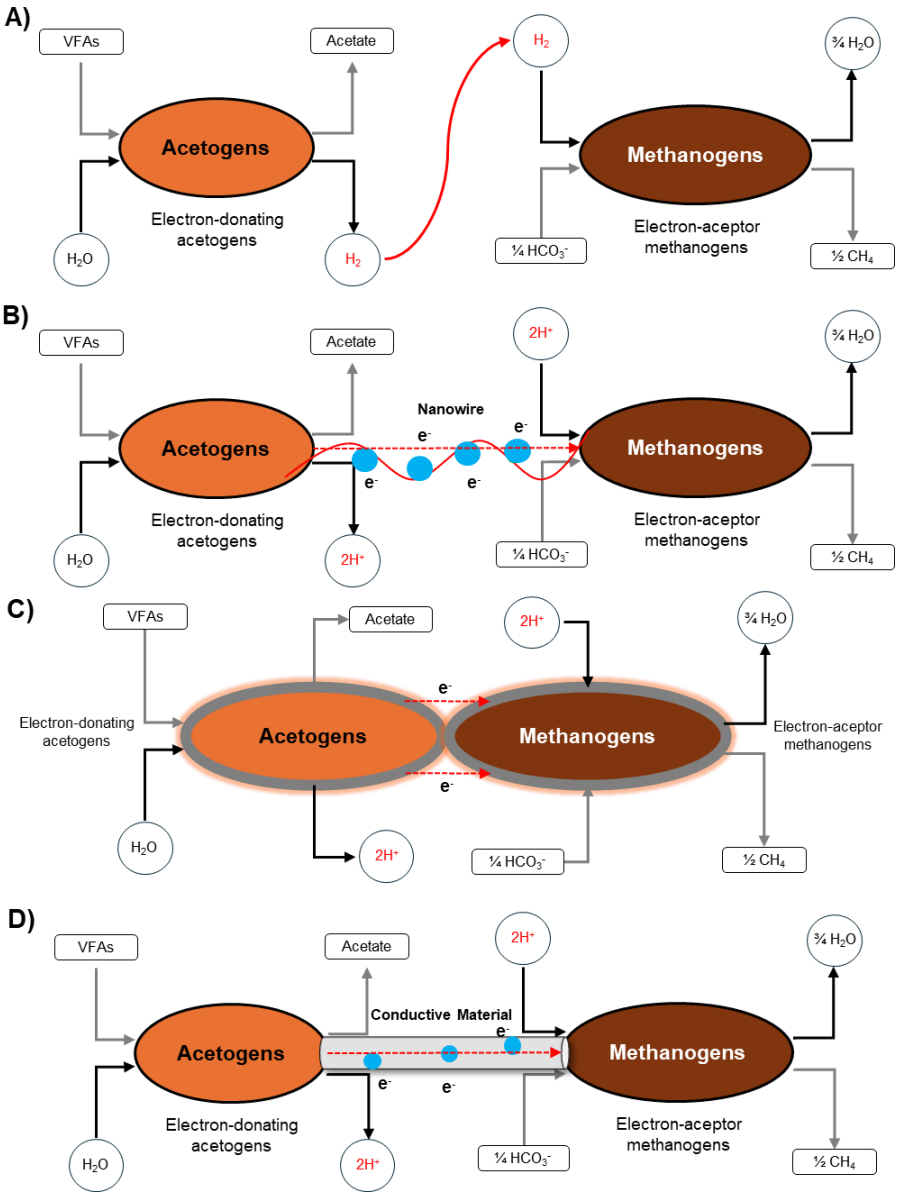

Figure 2. Electron transference pathways (A) Electron transfer via hydrogen, and DIET processes. (B) DIET via Conductive nanowire. (C) DIET via biological Electrical Connections at the Outer Cell Surface. (D) DIET via Conductive Materials.

1.4 Nickel-base conductive material for DIET

As mentioned above, that addition of non-biological conductive materials offers many advantages, thereby many conductive materials have been tried and used to enhance DIET process in AD. In recent years, using nickel as a conductive material for DIET has also been researched. There are numerous advantages to using nickel in AD. Nickel is not only a crucial trace element for the growth of bacteria and archaea, but it also exhibits a significantly higher electrical conductivity compared to carbon-based materials and iron, while its ecotoxicity is much lower than copper (Guo et al., 2020). One of the studies shows that the addition of nickel nanoparticles (17 nm, 2 mg/L) to the anaerobic digestion process significantly enhances biogas production, achieving a 70% increase under mesophilic conditions (Kumar et al., 2021). In addition, Ni was found to enhance methane production and influenced the dominant archaeal populations in anaerobic digestion processes treating food industry waste (Feng et al., 2010). Further studies have found that an addition of 2 mg/L nickel nanoparticles is the most effective concentration for enhancing methane production (Abdelsalam et al., 2016). However overloading nickel concentration can cause the obvious toxicity to methanogens during the AD process, resulting in a reduction of the AD process efficiency due to the disintegration of microbial cell membranes (W. Zhang et al., 2015d), (Kaur et al., 2021). Therefore, it is important to apply an optimal concentration when using nickel as conductive material in AD. Optimal concentration can significantly enhance the AD performance, while overloading can lead to system failure.

1.5 Problems statement

As discussed earlier, the addition of CMs into anaerobic digesters could promote the DIET mechanism, which can significantly boost AD efficiency performance, even when high OLR condition is supplied to the reactor. This promising approach has resulted in numerous research incorporating CM in continuous experiments, especially in up-flow anaerobic sludge blanket (UASB) reactors in the recent years. Despite the widespread use of UASB reactors for biologic wastewater treatment, several challenges were found when integrating CM into these systems.

1.5.1 Up-flow Anaerobic Sludge Blanket (UASB) reactor

The UASB reactor is designed for efficient performance and low-cost wastewater treatment by facilitating the granulation of AD sludge (Souza, 1986). This reactor offers numerous benefits, including efficient settling of granular sludge, which enables easy solid-liquid separation. This promotes effective performance in managing high OLR influences due to the close microbial interactions within the granules (Van Lier et al., 2010) (Bobade & Lomte, 2015). Given these advantages, researchers have explored the potential of incorporating CMs into the UASB reactors to achieve a higher AD performance in high OLR. However, the application of CM in UASB reactors poses a significant challenge regarding the retention of CM in the reactor. Due to the up flow of influent into the UASB reactor, CMs with small particle size tend to float easily leading to washout of CMs together with the effluent (Figure 3) (Kim et al., 2022) (Baek et al., 2018). The wash out of CMs not only limits the interaction of microbes and CM but also raises concerns on the additional costs for continuous replenishment and the risk of nano pollution. Therefore, retaining CMs within the UASB reactor is crucial to enhance the DIET mechanism in AD processes, while also preventing the additional cost associated with CM replenishment and mitigating secondary nano pollution.

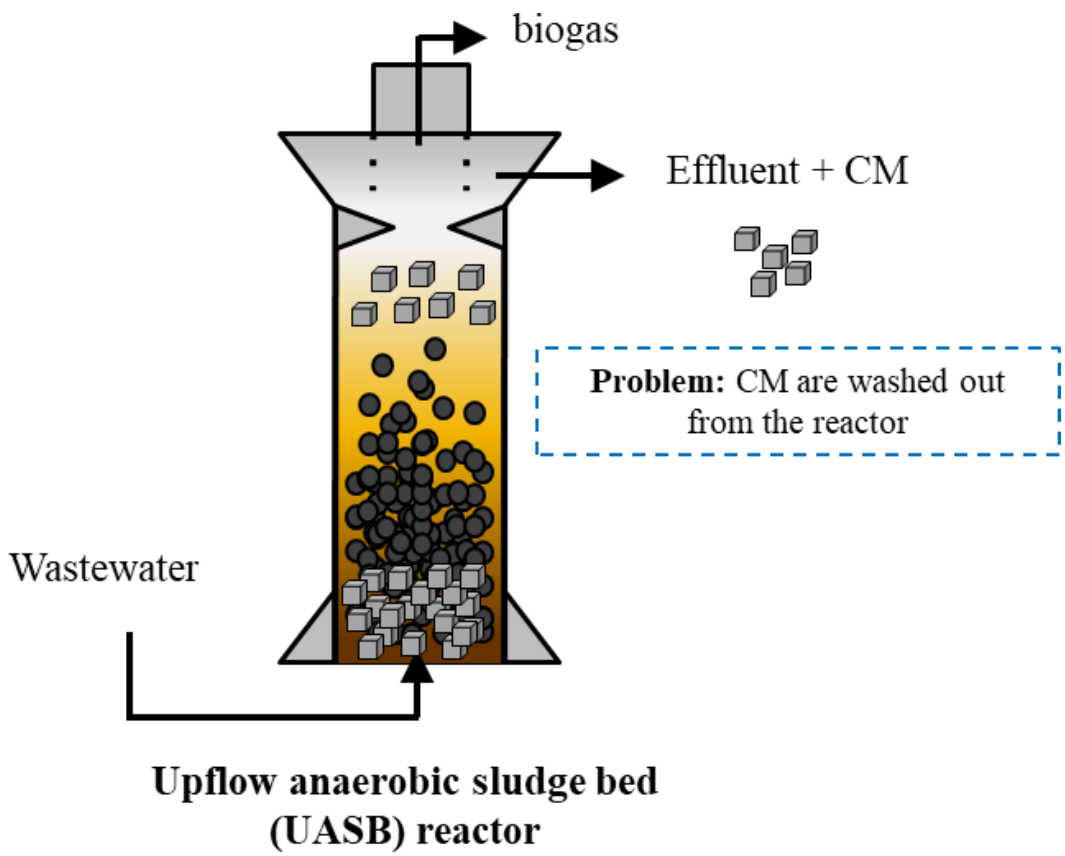

Figure 3. Challenges in adding conductive materials to upflow anaerobic sludge (UASB) reactor.

1.6 Solution proposal

In recent years, the immobilization of microbial cells has become prevalent in biological wastewater treatment, owing to its advantages. These include augmenting biomass, enabling cell reuse, enhancing resilience to toxic chemicals, and mitigating the wash-out of CMs (Bouabidi et al., 2018). One of the methods attracting considerable attention for immobilizing biomass is the utilization of sponges as immobilization carriers. It has been studied that immobilizing microbes on sponges could retain most of the microbes in the bioreactor and improve the biotreatment process (Yang et al., 2004b). Therefore, studies on using Nickel Foam in AD experiments have also been made to not only enhance methane production rate through the DIET mechanism, but also prevent washout of CM (Li et al., 2021). However, its high production cost makes it less feasible for widespread use in cost-sensitive applications such as in the AD process. Therefore, this study proposes the use of a nickel-coated sponge as a carrier for CM instead of using a solid nickel sponge. By using the nickel-coated sponge, not only the washout of CMs from the reactor can be prevented, but since the carrier itself is conductive, it is expected that DIET could occur efficiently through easy microbial attachment on the sponge (Figure 4). Additionally, compared to using solid nickel sponges, this approach leverages the cost advantages of coating nickel and the structural benefits of the sponges, making it a practical and scalable solution for improving the efficiency of AD process. However, several factors such as the sponge material and coating method must be carefully considered to synthesize a cost-effective nickel coated sponge.

1.6.1 Sponge carrier

Polyurethane sponge (PS) has been widely tried to enhance different biological wastewater treatment performance, and it is one of the most used sponge materials added to the anaerobic digestion (AD) process. This sponge presents characteristics such as its high porosity and high specific surface area for biomass attachment, and its exceptional

durability, which allows it to be used in for long periods (Tawfik et al., 2012). On the other hand, Melamine Sponge (MS), which is also known for its low cost presents a higher surface area compared to PS. This characteristic potentially enhances the immobilization of microbes more efficiently than PS, leading to higher biogas production rate in the AD process. However, MS exhibits lower durability compared to PS and has limited applicability in the field of wastewater treatment. The limited use of MS raises unanswered questions regarding its performance in biological processes and the potential for inhibition in the metabolism of AD microbes, which could disrupt the operation. Therefore, both sponges will be trialed in this study to determine a suitable sponge carrier for AD process.

1.6.2 Nickel coating method

Nickel plating constitutes a process with multifaceted advantages, including corrosion prevention, enhancement of hardness and strength, augmentation of wear resistance, and enhancement of product aesthetics (Mazur et al., 2018) (Gezerman & Corbacioglu, 2010). There are many coating techniques such as using chemicals, hot-dip galvanizing, thermal spraying, diffusion, and many more. However, such techniques require high equipment expenses and limitations in shaping metallic parts. In contrast, electrochemical methods are widely favored in industry for their practicality and lower costs (Mazur et al., 2018).

The nickel-electroplating process provides coatings with minimal internal stress, high ductility and enhances the conductivity of materials, making them more suitable for various industrial uses. Despite being a cheaper process than the ones mentioned above, nickel electroplating still requires careful control of additives and current density during deposition to ensure optimal properties and cost-efficiency (Agboola et al., 2018).

On the other hand, with no electricity required, electroless nickel plating offers the advantage of being conducted in a controlled environment with reduced equipment

requirements compared to traditional electroplating. Additionally, this method achieves a durable and high-quality coating presenting a uniform Ni deposition and fewer application layers, providing a feasible alternative to the usual electroplating (Loto, 2016). Thereby, based on this knowledge, this study will utilize the electroless plating method for coating the sponges. Sponge plating using the Ni-electroless plating method could offer a financially viable option, combining both a carrier and a highly conductive material to enhance DIET in the AD process.

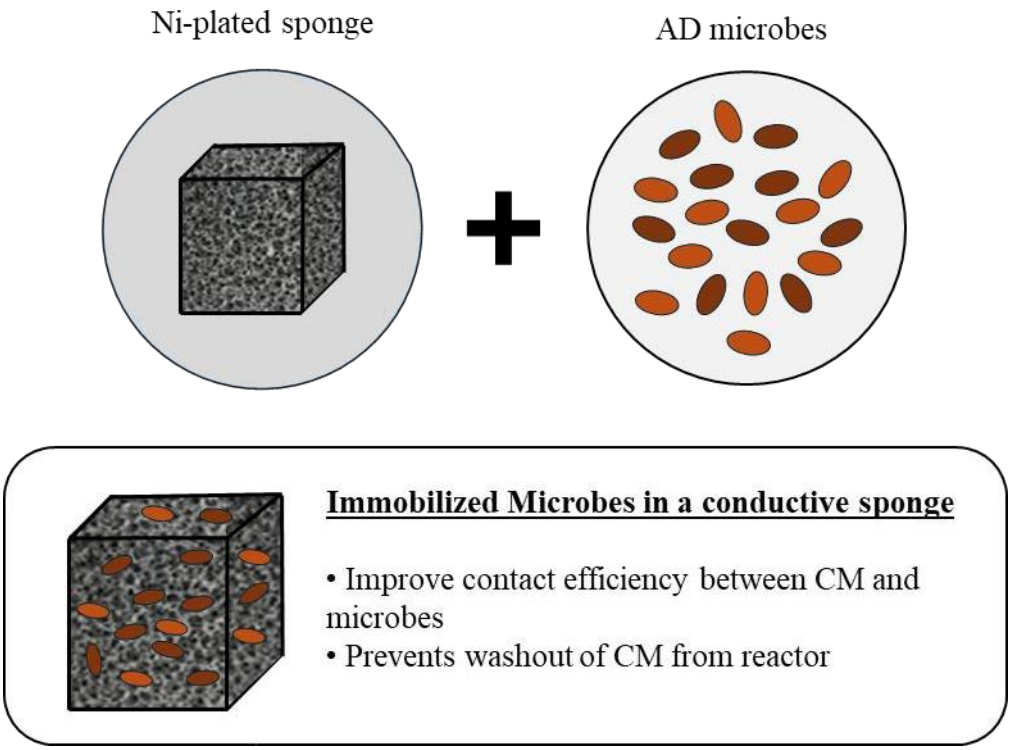

Figure 4. Proposal of using a nickel-plated sponge to immobilize anaerobic digestion microbes

1.7 Research objective

The main objective of this study is to evaluate the nickel coated sponge, produced via the electroless plating methods, in anaerobic digestion process. Nevertheless, before directly addressing this research, several smaller factors must be investigated. Thereby, the objective of this study is divided into the following experiments:

1. Evaluating Melamine Sponge's biotoxicity in anaerobic digestion process.
2. Trial in plating nickel on polyurethane sponge and melamine sponge via electroless plating method.
3. Evaluating nickel plated melamine sponge and polyurethane sponge for selection as immobilizations carrier for anaerobic digestion experiment.
4. Evaluating continuous anaerobic digestion performance with the addition of nickel-plated sponges in UASB reactor.

Chapter 2: Evaluating Melamine Sponge's biotoxicity in anaerobic digestion process.

2.1 Background/Overview of Experiment 1

In the field of wastewater treatment, sponge carriers are known for their potential to immobilize microbes, significantly enhancing the performance of various bioreactors. For instance, they have been widely reported to increase the efficiency of nitrogen removal in membrane bioreactor (MBR) (Kurita et al., 2016), eliminate ammonia from synthetic freshwater Return Activated Sludge (RAS) wastewater (Shitu et al., 2020), and achieve high-rate nitrogen removal from anaerobic digester liquor in an up-flow anammox reactor (Zhang et al., 2011). Polyurethane sponge (PS) has been extensively studied in different biological organic waste treatment processes and has been reported as an efficient option for biomass attachment, enhancing the wastewater treatment performance (Chen et al., 2022).

On the other hand, the use of melamine sponge (MS) which is known for its cheap cost and high surface area is limited in biological wastewater treatment. Its high surface area characteristics are expected to immobilize the microbes more effectively than PS allowing them to form biofilms attached to the sponges' pores. This could potentially lead to a higher biogas production rate in the AD process. However, given the limited use of MS, there is a lack of knowledge regarding its performance in biological processes as well as the possibility of causing inhibition in the metabolism of AD microbes, which could disrupt the operation.

Taking all these factors into account, a preliminary experiment was conducted to assess whether the use of MS poses a potential risk for inhibiting the AD process. Process performance was evaluated by measuring daily biogas production, pH, the Volatile Fatty

Acids (VFAs) and ethanol's concentrations and the sponge's durability. This experiment will help to determine the suitability of using MS in subsequent AD experiments.

2.2 Materials and methods

2.2.1 Experimental set up

For the experiment set up, two medium glass bottles of 0.5 L were used as reactors and operated for 16 days in batch mode. The reactors were placed in a thermal bath at 37ºC and connected to different gas bags to collect daily produced biogas. Anaerobic sludge obtained from the Hakubu Sludge Treatment Centre (Yokohama, Japan) was used to prepare two different conditions: 1) 300 mL of anaerobic sludge with no addition of sponge as "Control" and 2) the same volume of sludge with an addition of 200 mL of MS as "Melamine sponge" condition. The MS (Melamine sponge, 3 × 3 × 3 cm; Okazaki, Japan) were cut into 1 cm^3 blocks by using a cutter and were squashed in the reactor with a spatula for 5 min to promote sludge absorption into the sponge and avoid flotation of the sponges. Ethanol was used as the substrate with an inoculum-to-substrate ratio of 2:1 Volatile Solid (VS) base. Table 1 shows the Total Solid (TS) and volatile solids contents in the inoculated sludge where VS value is 18.116 g-VS/L, thereby 1.647 mL of ethanol was added to each reactor. The reactors were stirred at 600 rpm by using a magnetic stirrer to maintain uniform distribution of substrate throughout the reactor. Sampling was done every 3 days, for volatile fatty acids (VFAs) and ethanol measurement, as well as the pH in the reactor. Before the experiment, each reactor was purged with N_2 for 1-2 min to ensure an anaerobic environment. The reactors were purged again each time they were opened for sampling.

2.2.2 Analytic methods

Total Solids (TS) and Volatile Solids (VS) were measured before the experiment using the methods from the American Public Health Association (American Public Health Association, 2005). In brief, three different sludge samples of approximately 5 mL were placed in small aluminum paper dishes and weighted before and after adding the sludge. The samples were heated to 105ºC for 2h to remove the water and weighed to obtain the

TS value. Then, they were subjected to 550ºC to remove the VS, and the remaining ash was weighed together with the dish. The VS was calculated by subtracting the weight after 550ºC from the weight after 105ºC.

The biogas was collected from the gas bags every day, and its volume was measured manually by using a 60 ml syringe. Then, the biogas was then introduced into the CO_2 absorption unit to measure the percentage of CH_4 in the biogas. The CO_2 absorption unit was prepared as follows, in brief 5 ml of 0.4% thymolphthalein pH-indicator solution was added to 1L of the 3M NaOH solution. The daily produced biogas was purged into a bottle containing this mixture. The CO_2 is stripped from the biogas allowing the CH_4, which did not react with the solution, to be recovered in another 60 ml syringe.

In every sampling, the samples were centrifuged at 4000 rpm for 15 min to collect the supernatant, and then was filtered using a glass fiber filter (GC-50, 47mm; ADVANTEC, Japan) and stored at below -20℃ until further analysis. Ethanol and VFAs were analyzed using gas chromatography with a flame ionization detector (FID) (Shimadzu Gas Chromatography, GC-2014) equipped with a BX-100 60/80 glass column and a Unisole F-200 30/60 glass column. For analyzing ethanol, the injector, detector, and column temperatures were maintained at 250°C, 110°C, and 110℃, respectively, with nitrogen used as the carrier gas at a flow rate of 32 mL min^{-1}. For analyzing VFAs, the injector, detector, and column temperatures were maintained at 200℃, 140℃, and 140℃, with nitrogen used as the carrier gas at a flow rate of 35 mL min^{-1}. pH was measured using a pH meter (Bettler Toledo, S220-Basic).

As for the evaluation of the biomass attachment on the sponge, one sponge was collected from the reactor every day to measure its weight and screen any physical damage on the sponge.

2.2.3 Methane production rate data analysis

Since microbial activity is linked to biogas production, the cumulative methane gas production was analyzed using the modified Gompertz model equation (Equation 1) to determine the methane production rate and the lag phase. The modified Gompertz model equation is as follows:

$$f(t) = P \times exp\ (-exp\ (\frac{e \cdot Rm}{P} \times (l - t) + 1)\ )\ \text{(Eq.1)}$$

where $f(t)$, P, Rm and l represent the cumulative methane production at time *t*, the maximum cumulative methane production at the end of the incubation period, the maximum methane production rate, and the lag phase, respectively.

Table 1. Preliminary experiment sludge TS-VS concentration

	Total Solid (g-TS/L)	Volatile Solid (g-VS/L)
Sludge	24.601	18.116

2.3 Results and discussion

2.3.1 Characteristics of melamine sponge throughout the AD experiment

Throughout the experiment the sponges were expected to increase in weight every day due to biomass attachment. Therefore, the sponges were weighed daily to determine the duration for maximum biomass to be immobilized on the sponges. However, only after day 1, the sponge can be seen to be broken down into smaller pieces (Figure 5-A). The sponges continuously become smaller by day, and from day 4 onwards, no physical sponges could be found in the reactor (Figure 5-B). This was attributed to the fragility of the MS which was easily broken down due to the friction caused by the high stirring rate (600 rpm) in the reactor. This hypothesis was confirmed by conducting a trial experiment in which three samples of MS are placed in a conical beaker containing MQ water and stirred at the same rate for a duration of 15 days. The result shows the same trend as the above result where the MS was broken down into smaller pieces by day (Figure 6). Although the sponge was not completely broken down in this trial experiment, it can be hypothesized that increasing the sponges used in the experiment will increase friction among them due to the confined space, thereby accelerating the breakdown. Therefore, the MS was concluded to be unsuitable to be used with a magnetic stirrer or stirring reactor. As a result, other types of AD reactors should be tested to assess the MS's resistance. Thus, the durability of MS was evaluated in a UASB reactor for 17 days (Figure 7-A), as this reactor does not require any stirring and is intended for use in a future continuous experiment. Following this trial the shape of the sponges remained the same as the first day, concluding that MS can be used in a UASB reactor (Figure 7-B, C).

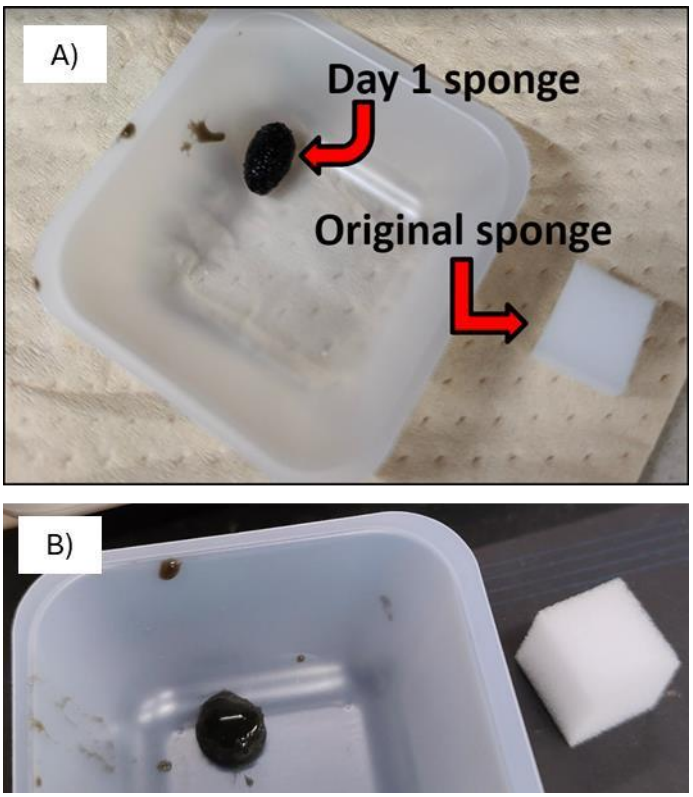

Figure 5. Shape changes of melamine sponge in anaerobic digestion experiment on A) day 1 and B) day 3

Figure 6. Comparison of original melamine sponge size and after 15 days of trial in MQ water.

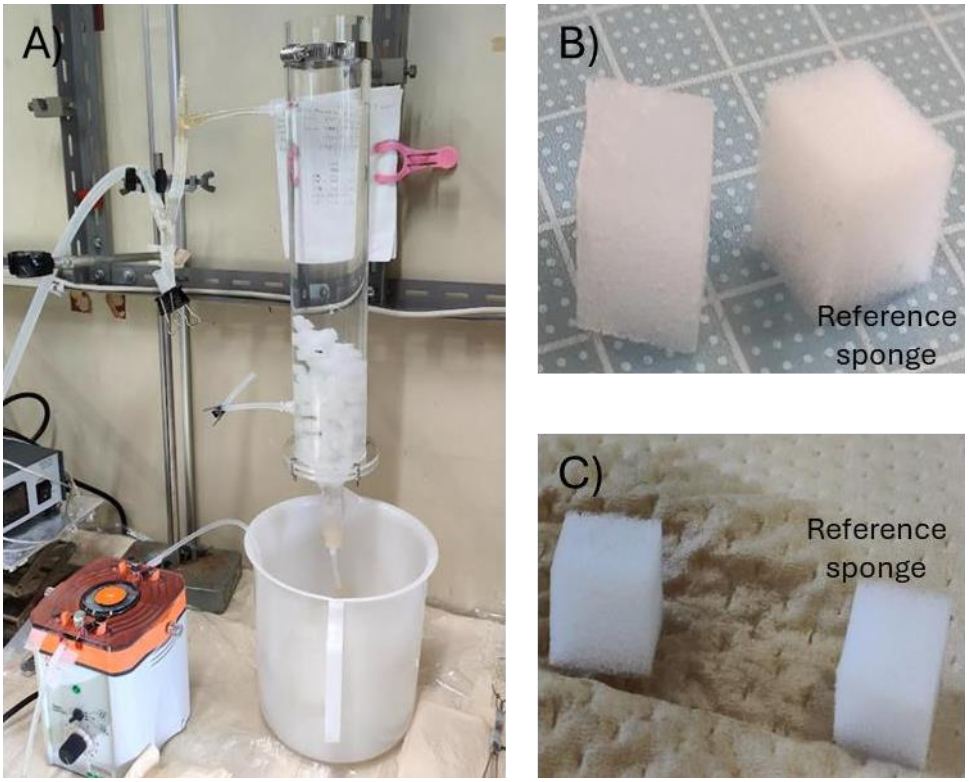

Figure 7. A) Trial of melamine sponge in UASB reactor. Melamine sponge shape in B) before and C) after the experiment

2.3.2 Biomethane batch experiment

The result of cumulative biogas and methane gas production for this preliminary experiment is shown in Figure 8. At the end of the experiment, both reactors exhibited the same cumulative biogas production, indicating that all the ethanol was utilized during the AD process and no inhibition was observed by the addition of MS. Based on this result, it can also be inferred that despite sponge breaking down (Figure 5), microbes did not utilize the MS as a substrate. In addition, past studies have also shown that melamine can be broken down by only aerobic microbes, thereby the breakdown of MS was unlikely utilized by AD microbes (Xu et al., 2017. Hatakeyama et al., 2015). During the first two days no significant difference in biogas production was observed. However, from day 3 onwards, the reactor with the addition of MS showed higher biogas production. The increase of production in "melamine sponge" condition can be attributed to the biomass immobilization in the sponge. In past studies, addition of zeolite (0.25-0.50 mm) for immobilizing AD microbes had a significant influence on methane production due to its tridimensional microporous structure, which allows microbes to adhere to the sponge (Fernández et al., 2007). Even though the sponges were broken down, the microbes may still be able to immobilize onto the broken smaller carrier just like the properties of zeolite. Figure 9-A shows the result of ethanol concentration. The result shows no significant difference between the control and the melamine sponge condition. On the other hand, the acetate concentration (Figure 9-B) shows that MS presents the highest peak at day 3 and it is completely degraded by day 9, while control shows the highest peak on day 6 and it is completely degraded by day 12. This result can be attributed to the immobilization on the sponges, which could help increase the intermediate transfer rate due to close contact between microbes, thereby showing the intermediate substrate (acetate) to be broken down faster compared to the control. Also, the pH result (Figure9-

D) shows that all the conditions are in the range of pH 7.47 – 8.25, which suggests that AD proceeded smoothly with no inhibition (Yang et al., 2015).

To obtain the methane production rate result, the value from Figure 6 was fitted into the Modified Gompertz equation (Eq.1) and the results are also shown in Table 2 and Figure 10. The melamine sponge condition shows a higher maximum production rate with 234.69 mL/g-COD/day, which is 1.11 times faster than the control condition. Additionally, the MS condition also shows a shorter lag time of 1.6 days compared to control with 2.4 days, demonstrating that the addition of MS can enhance the efficiency initiating the conversion of acetate into methane.

It should be noted that the maximum cumulative methane gas production was 564 mL-CH_4/g-COD which is way over the theoretical methane gas per COD (1 g COD = 0.35L) (Tauber et al., 2019). This may be due to the generation of propionate acid in both reactors (Figure 9-C). Although only ethanol was used as substrate in this preliminary experiment, the production of propionate acid was observed. This may be due to the residual of organic matters from the sludge center. During the batch experiment, the remaining organic matter taken from the sludge center was converted into propionate acid, thereby showing a higher cumulative methane gas production at the end of the experiment.

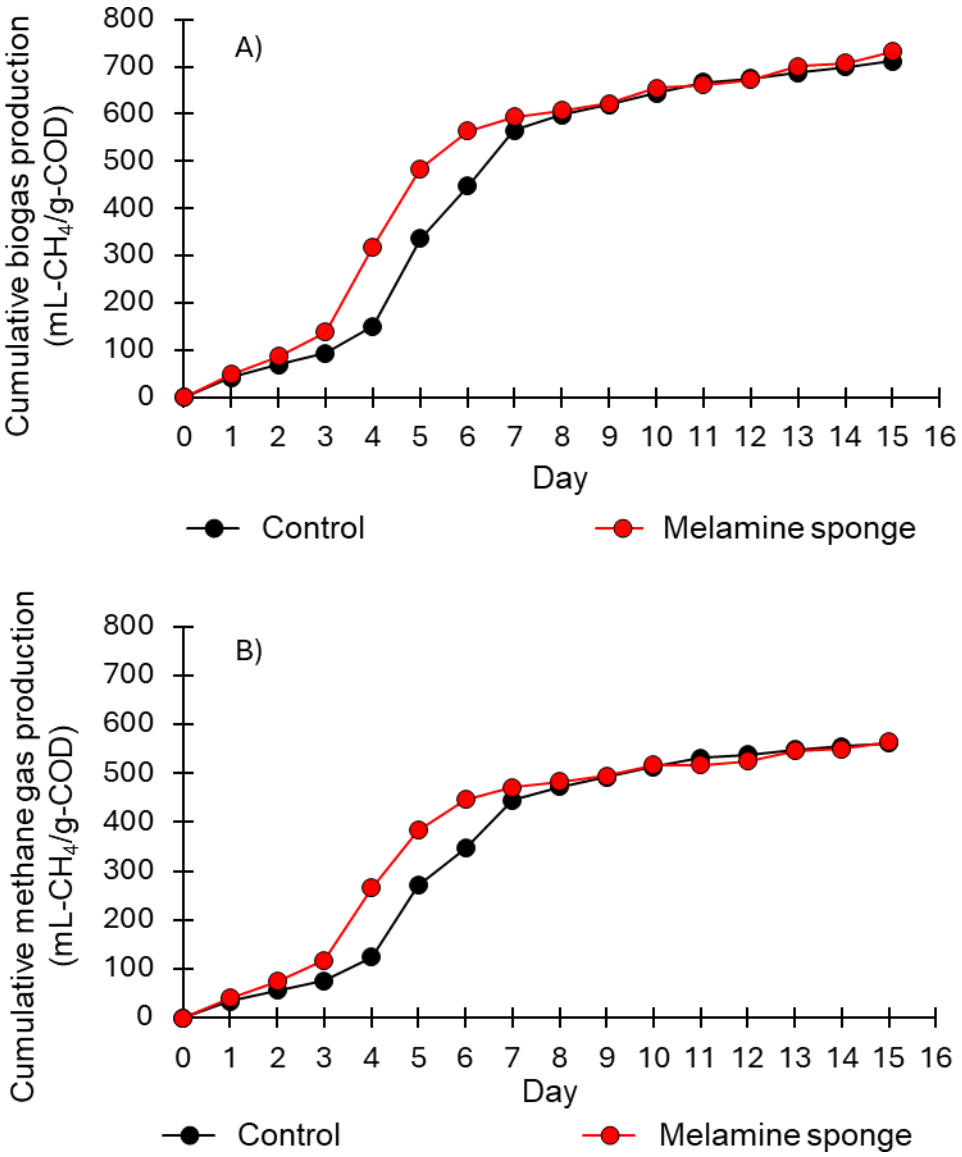

Figure 8. A) Preliminary experiment cumulative biogas production, B) Preliminary experiment cumulative biogas production

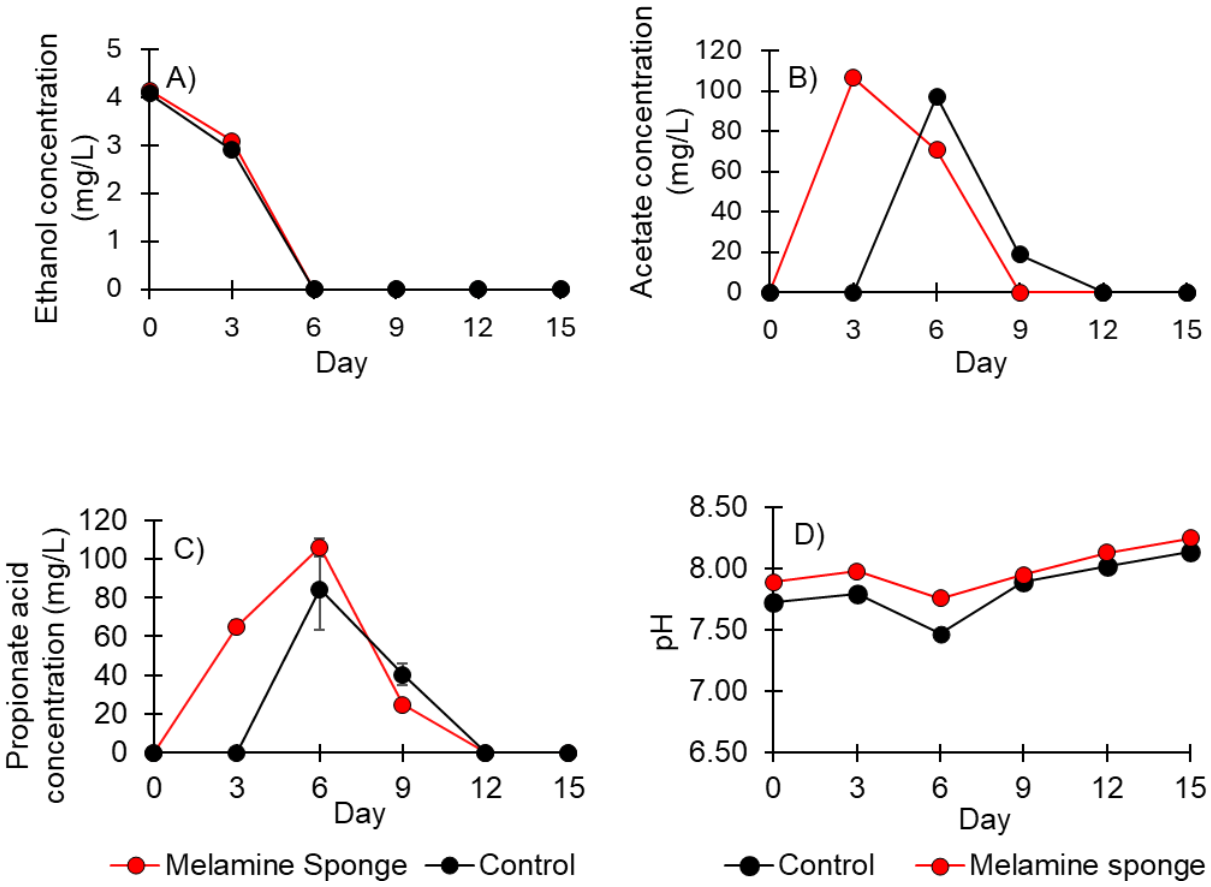

Figure 9. A) Ethanol concentration, B) Acetate concentration, C) Propionate acid concentration and D) pH throughout the preliminary experiment

Table 2. Kinetic parameter from preliminary experiment result fitted into the Gompertz equation.

	P (mL/g COD)	Rmax (mL/g-COD/day)	l (day)	R^2
Melamine sponge	1124.792	234.692	1.634	0.991
Control	1165.157	210.662	2.412	0.993

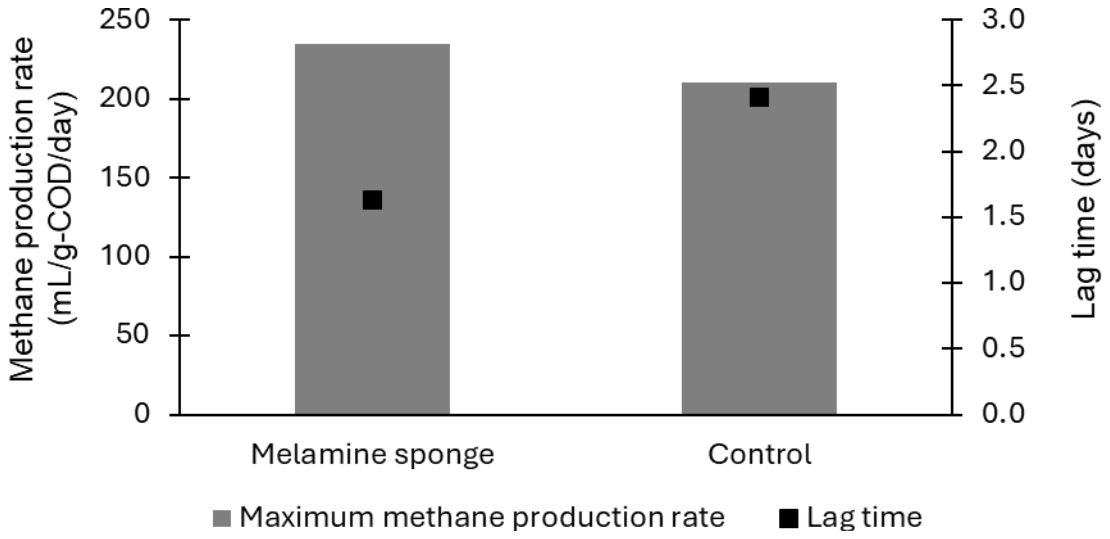

Figure 10. Methane production rate and lag time of the preliminary experiment

2.4 Conclusion

In this chapter, the performance of MS was evaluated in the anaerobic digestion batch process. The results indicate that MS exhibits no biotoxicity that could negatively affect microbial metabolism. On the contrary, the addition of MS could enhance the methane production rate by 1.11 times and reduce the lag phase by 0.8 days compared to the control condition. However, it was confirmed that MS is not suitable to be used with a stirring reactor due to its poor durability which will lead to sponge breaking down through friction easily. Nevertheless, the trial in the UASB reactor was successful, where the MS maintained its shape even after 17 days. Thereby, the UASB reactor will be used in the future study.

Chapter 3. Evaluating electroless nickel plating on Polyurethane Sponge and Melamine Sponge

3.1 Background/Overview of Experiment 2.

In the field of DIET research, one of the challenges left unsolved is the washout of CM from the reactor. To solve this problem, previous studies have used Nickel Foam as CM to solve the washout problems and shown promising results on DIET (X. Guo et al., 2020). However, synthesizing nickel foam has a disadvantage of high-cost production and may produce more secondary wastewater. On the other hand, the electroless nickel plating method can be done in a more controlled environment with less equipment and requires fewer coats to produce a strong high-quality coating, resulting in a higher cost-effective process. Additionally, the electroless plating method provides a uniform coating with excellent corrosion and wear resistance, anti-galling properties, and versatility for diverse applications, making it ideal for complex geometries and harsh environments (Loto, 2016).

In Chapter 2, we concluded that there is no biotoxicity from the melamine sponge (MS) toward the anaerobic microbes. On the other hand, as mentioned in Chapter 2 too, Polyurethane sponge (PS) has been used in numerous studies in various biological organic waste treatment processes as it could effectively promote biomass attachment on the sponge and has proven to significantly enhance wastewater treatment efficiency (Chen et al., 2022). However, it is unknown if these materials are suitable for plating nickel using the electroless plating method. Therefore, in this study, trials on plating nickel on MS and PS using the electroless plating method will be conducted, to evaluate its potential application in the subsequent AD experiment. The plating method will be assessed on a small scale, with the goal of preparing a large quantity of the sponges for the continuous experiment in a single batch.

3.2 Materials and methods

3.2.1 Solutions preparation and maintenance

The solutions and methods needed for electroless nickel plating were generously provided by Hikifune Co., Ltd, Japan. Before plating the sponge, the following 5 solutions were prepared along with the maintenance information as stated below. It should be noted that after every plating batch was done, solutions were filtered with a filter paper (90 mm; ADVANTEC, Japan) and maintenance was done to have the same concentration and achieve the same plating efficiency for the next plating batch.

Solution 1 (Alkaline degreasing):

The first solution was prepared by adding 10 g of E-33 Cleaner (Atotech, Japan) into 200 mL MQ water to achieve concentration of 50 g/L. The solution was stirred until the solute was completely dissolved.

To achieve an efficient plating, maintenance of the solution was done after every plating. To maintain the alkaline degreasing solution; 10 mL of solution 1 was poured into a conical beaker, then 3 drops of methyl orange indicator were added. The solution was then titrated with 1N H_2SO_4 until the color of the solution changes from orange to pink. Solution's concentration was determined by the following equation:

$$V_{H2SO4}\,(mL) \times 5.63 = \text{Concentration of E-33 solution (g/L)} \quad \text{(Eq.2)}$$

where V_{H2SO4} is the volume of H_2SO_4 titration in mL. Based on the methods given by Hikifune Co., Ltd, Japan, the concentration range for solution 1 should be in between 50-100 g/L, while 50 g/L is known to be the most favorable concentration for the plating performance.

Solution 2 (Etching solution):

This second solution was prepared by dissolving 52 g of TOP Piena 300 Pre-dip (TOP Piena Process, Okuno Chemical Industries Co., Ltd, Japan) salt into 200 mL of MQ water to achieve the concentration of 260 g/L. Solution was continuously stirred until completely dissolved.

As for the maintenance, 20 mL of solution 2 was first poured into a conical beaker, proceeding by adding 3 drops of phenolphthalein indicator. The mixture was titrated with 1 mol/L NaOH until the solution turned pink. The concentration of the solution was determined by the following equation:

$$V_{NaOH}\,(mL) \times 42.13 \times F^{*} = \text{Concentration of Etching solution (g/L)} \quad \text{(Eq.3)}$$

where $V_{NaOH\ is}$ the volume of NaOH titrated in mL and F^{*} is the factor of 1 mol/L NaOH solution. The concentration range was listed to be between 240-280 g/L, where 260 g/L is the most favorable concentration for the plating performance.

Solution 3 (Catalyst solution):

The third solution was prepared by dissolving 52 g of TOP Piena 300 Pre-dip (TOP Piena Process, Okuno Chemical Industries Co., Ltd, Japan) salt into 191 mL of MQ water to become 260 g/L . Once the solution is completely dissolved, 9 mL of TOP Piena 400 Catalyst (TOP Piena Process, Okuno Chemical Industries Co., Ltd, Japan) was added to achieve a concentration of 45 mL/L. Solution was continuously stirred until the mixture reached a homogenous state.

As for the maintenance, 5 mL of solution 3, 5mL of 35% hydrogen peroxide solution and 20 mL of 6 mol/L hydrochloric acid are added in a 250 mL volumetric flask. Then MQ water was added to achieve the final volume of 250 mL. The mixed solution

was then measured in the Ultraviolet-Visible spectrometer (UV–Vis) (V-650 Series, JASCO, Japan).

The concentration range is listed to be from 0.1-0.23 g/L, where 0.19 g/L is the most favorable concentration for the plating performance.

Solution 4 (Accelerator solution):

Solution 4 was prepared by adding 20 mL of TOP Piena 500 Accelerator A (TOP Piena Process, Okuno Chemical Industries Co., Ltd, Japan) to 160 mL of MQ water into a beaker and stirred until homogenized. Then, 1.6 ml of TOP Piena 500 Accelerator B (TOP Piena Process, Okuno Chemical Industries Co., Ltd, Japan) was added and stirred until the mixture reached a homogenous state.

As for the maintenance, 10 mL of the accelerator solution was poured into a beaker of 100 mL of MQ water, followed by adding 3 drops of phenolphthalein indicator. The mixture was titrated with 1 mol/L NaOH until the solution turns pink. The concentration of the solution was determined by the following equation:

$$V_{NaOH}\,(mL) \times 7.24 \times F^{*} = \text{Concentration of Accelerator solution (mL/L)} \quad \text{(Eq.5)}$$

where $V_{NaOH\,is}$ the volume of NaOH used in titration in mL and F^{*} is the factor of 1 mol/L NaOH solution. The optimal concentration range was listed to be from 85-130 ml/L, where 108 ml/L is the most favorable concentration for the plating performance.

Solution 5 (Electroless Ni-plating):

The electroless Ni plating solution was prepared by first adding 400 mL of MQ water to a volumetric flask. Then 50 mL of TOP Nicoron BL-M (TOP Nicoron BL, Okuno Chemical Industries Co., Ltd, Japan) and 30 mL of TOP Nicoron BL-1 (TOP Nicoron BL, Okuno Chemical Industries Co., Ltd, Japan) solutions are added respectively.

The volumetric flask was then filled with MQ water until the total volume reached 500 mL.

The concentration was evaluated by a maintenance process as follows; 5 mL of solution 5 was first transferred to a conical beaker, then 80 mL of MQ water and 10mL of ammonia water and 0.1-0.2g of murexide (MX) are added respectively. The solution was titrated with 0.05 mol/L-EDTA standard solution until the color changes from greenish-yellow to reddish-purple. The solution's concentration was determined by the following equation:

$$V_{EDTA}\,(mL) \times 0.587 \times F^{*} = \text{Concentration of Ni plating solution (g/L)} \quad \text{(Eq.5)}$$

where V_{EDTA} is the volume of EDTA used in titration in mL and F^{*} is the 0.05mol/L-EDTA standard solution factor. The optimal concentration range was listed to be from 4.1-6.9 g/L, where 5.5 g/L is the most favorable concentration for the plating performance.

3.2.2 Electroless plating method.

Initially, a small-scale experiment was conducted using three MS (Melamine sponge, 3 × 3 × 3 cm, Okazaki, Japan) and three PS (Aquaporusgel, 426mm^3, Nisshinbo Chemical Inc., Japan) to test the electroless Ni plating method on both sponges. To ensure uniform plating condition, all 6 sponges (3 MS & 3 PS) were plated together in this trial experiment. The following outlines the procedural steps of the electroless plating method and the function of each process. For better clarity, a schematic representing the electroless nickel plating process is provided in Figure 11. In brief, all six sponges (three MS & 3 PS) were introduced into solution 1 (alkaline degreasing solution) at 50 ºC for 5 mins. This step is employed to remove any possible contaminant on the sponge and improve its wettability for the subsequent etching process. The sponges were squeezed in the solution using a muddler to remove air bubbles and for solution to penetration inside the sponge. This same method was used when sponge was introduced into solution 2, 3 and 4. After 5 min, the sponges were taken out using a net, and any excess solution was gently squeezed out. The sponges were cleaned with RO water three times and were gently squeezed to remove excess water. Next, the sponges were transferred to solution 2 (etching solution) at 30ºC for 2 min. This step is to etch the material of the surface to add hydrophilic properties to it. After 2 min, the sponges were taken out and cleaned with RO water 3 times, the same way as stated in the above. Then, the sponge was transferred to solution 3 (catalyst solution) for 3 min at 30ºC. This step is to add a palladium catalyst to the sponge surface by absorbing Pd-Sn colloid onto the sponge. The sponges were cleaned with RO water in the same way as stated on the above after 3 min, and then transferred into solution 4 (accelerator solution). This step is used for surface adjustment by removing Sn from the sponge. Sponges were treated at 30ºC for 3 min in solution 4 before cleaning it with RO water 3 times, before being transferred into a room temperature solution 5 (Electroless Ni-plating) as a preliminary step. Once the solution 5 was

thoroughly absorbed by the sponge at room temperature, the sponge was transferred into solution 5 which was heated at 90ºC and was treated for 10 min. In this step, electroless nickel plating will be deposited with Pd as the reaction catalyst nucleus. The preliminary step was to ensure even more efficient plating. Also, it should be noted that electroless plating can only be performed when Ni solution is between 85-95ºC, therefore it is important that solution 5 stays constant at 90 ºC when the sponge is introduced until the treatment is over. In addition, since hydrogen is produced during the plating treatment, a chopstick was used to gently shake each sponge for bubbles (hydrogen gas) to be removed and for uniform plating. Wood chopsticks were used to prevent the reaction of the Ni plating solution on the tool. Lastly, after being treated for 10 min, sponges were taken out and rinsed several times with RO water and put in the oven at 80ºC for 2 hr. It should be noted that for the last cleaning using RO water, the sponges were not squeezed as the nickel plated on the sponge could be peeled off.

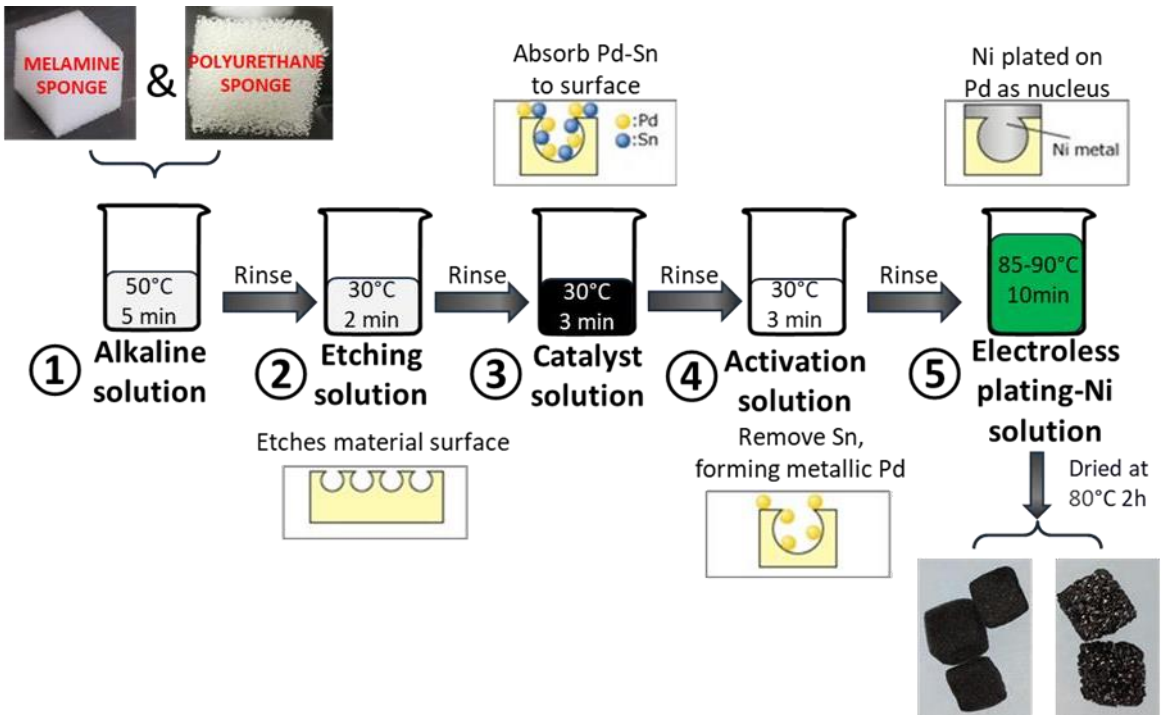

Figure 11. Schematic of Electroless Ni-Plating method process on melamine sponge and polyurethane sponge (ユケン工業株式会社, n.d.)

3.2.3 Analytical parameters

To evaluate the plating performance, all sponges were weighted before and after the plating batch. Specifically, the sponges were dried and weighed using a high-precision balance (Pheonix GH-252 Semi-Microbalance, A&D, Japan) before the plating process. After the plating process, the sponges were dried and reweighed again. The increase in weight corresponds to the nickel deposited on the sponge surface. Additionally, conductivity was evaluated after the electroless plating batch to ensure the success of the plating using a resistance (83 III MULTIMETER, FLUKE, USA) connected with 2-point electrodes. Different points were measured multiple times on each sponge to ensure uniformity of the plating. These evaluations are crucial for ensuring the quality and effectiveness of the plating process, thereby allowing for better understanding and optimization of the process.

3.3 Results and discussion

Figure 12 shows the image of MS and PS after electroless nickel plating. The result shows that both sponges were coated with Ni uniformly throughout the sponge and there was no significant change in shape after the Ni plating. Table 3 presents the average weights of the MS and PS sponges before and after plating. The results show that both sponges increased in weight, indicating successful nickel plating; however, the weight of the melamine sponges doubled after plating, whereas the polyurethane sponges only increased by 22.1%. In addition, the weight increase for both sponges shows particularly a similar value. Nevertheless, comparing it with the weight per sponge before plating, the melamine sponge shows a higher nickel deposition of about 18.3% higher compared to the polyurethane sponges. These results are probably due to the higher specific surface area of MS than PS, which allows more nickel to be deposited onto the surface of the MS. To determine if plating was successful, the conductivity of the sponges was also evaluated. Due to the instrumental noise, we could not obtain the current value as it is continuously changing and unstable, thereby could not provide any result. Nevertheless, both sponges had shown conductivity at all points even at different placement point measurements. This led to the conclusion that the electroless plating method was able to efficiently perform on both PS and MS sponges.

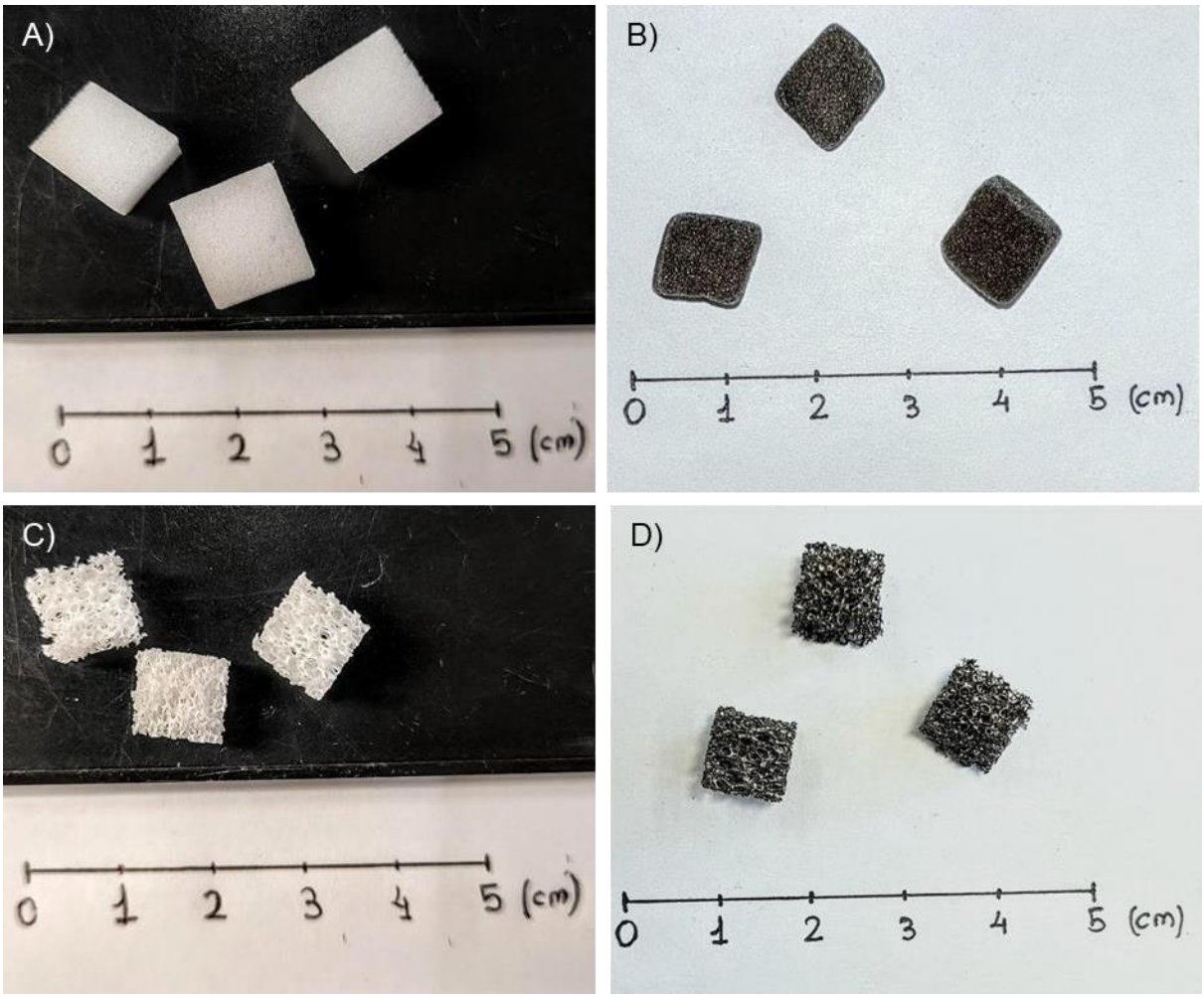

Figure 12. Morphology of A) MS before plating, B) MS after plating, C) PS before plating and D) PS after plating.

Table 3. Average weights melamine sponge and polyurethane sponges before and after electroless plating method.

Sponge	Weight per sponge before plating (g)	Weight per sponge after plating (g)	Nickel deposited on the sponge (g)
MELAMINE SPONGE	0.0092	0.0189	0.0097
POLYURETHANE SPONGE	0.0371	0.0453	0.0082

3.4 Conclusion

In this chapter electroless nickel plating method was tried on PS and MS to verify if the material is suitable to be plated on. The result demonstrated that nickel plating performance on both PS and MS sponges was successful, with MS sponges showing a higher nickel deposition (18.3% higher) which could be attributed to their larger surface area. Both types of sponges exhibited conductivity at all points, indicating successful plating. In the next chapter, further analysis of nickel-plated MS and PS will be conducted to select a suitable plated-sponge for the AD experiment.

Chapter 4. Evaluation of melamine and polyurethane sponge for selection in subsequent AD continuous experiment

4.1 Background/Overview of Experiment 3.

In chapter 3, trials of plating nickel on Polyurethane Sponge (PS) and Melamine Sponge (MS) using the electroless plating method were successful. Thereby, this chapter will further characterize the nickel-plated PS and MS to select the most suitable sponge for anaerobic digestion.

In this study, evaluation of biomass attachment on both plated sponges will be conducted. This evaluation is crucial as the DIET mechanism can only occur when DIET related microbes are attached together with conductive materials (L. Feng et al., 2023). This study seeks to determine which sponge can facilitate greater biomass attachment, thereby enhancing the DIET performance. Other parameters such as the Ni^{2+} release rate and the morphology of the sponges after the experiment will also be screened.

4.2 Materials and methods

4.2.1 Nickel sponge preparation

Both nickel plated MS and PS were prepared in the same way as written in chapter 3, section 3.2.2. After plating, the mass of the sponges was measured and compared with their initial weight. Additionally, the conductivity of the plated sponges was assessed to determine the success of the plating process.

4.2.2 Experiment set-up

Table 4 outlines all the experimental conditions used to evaluate the biomass attachment on the sponges. Specifically, three plated MS and PS samples were added to each of two separate 100 mL of AD sludge. To differentiate between tightly bound and loosely bound biomass attached on the sponges, an additional set of identical conditions from the above was prepared, with the modification of washing the sponges with phosphorus buffer saline (PBS) solution after the experiment. Furthermore, conditions with three plated-MS and PS samples in 100 mL of MQ water medium were prepared to screen for potential damage and any nickel coating that was peeled off the sponge. Additionally, an extra condition of adding non-plated(raw) MS and PS samples into 100 mL of AD sludge was also added to assess the effect of biomass attachment on before and after plating the sponge. All conditions were conducted in triplicate and were placed in a double shaker (NR-30 Double shaker, TAITEC, Japan) at the shaking speed of 160 rpm for 7 days. It should be noted that temperature was not controlled, nor substrate was supplied in this experiment as this study aims to evaluate the biomass attachment. In addition to that, 5 mL of sample was taken daily to evaluate the releasing rate of Ni^{2+}.

Table 4. Experimental conditions for sponge comparison

Condition Nº	Sponge	Ni plated	Medium	Washed with PBS
1	MS	Non-plated	AD sludge	x
2	PS	Non-plated	AD sludge	x
3	MS	Plated	AD sludge	x
4	PS	Plated	AD sludge	x
5	MS	Plated	AD sludge	o
6	PS	Plated	AD sludge	o
7	MS	Plated	MQ water	x
8	PS	Plated	MQ water	x

4.2.3 Analytic parameter

To assess the biomass attachment on the sponge, the sponges were weighed before and after the experiment. In detail, after the 7-day experiment, the sponges were dried at 105°C for 5 hrs and the sponges were weighted. The weight difference between before and after the experiment indicates the mass of Total solids (TS) attached on each sponge. To identify if any coated nickel was peeled off from the sponge, the medium was filtered with a glass fiber filter (GC-50, 47 mm; ADVANTEC, Japan) and dried at 105°C in the oven before weighing the filter at the end of the experiment. It should be noted that filtration was only done for conditions with MQ water medium.

As for analyzing the nickel ion release, all sample were measured in the ICP; Inductively Coupled Plasma machine (7850, ICP-MS, Agilent, Japan) after its pretreatment as follows: samples with AD sludge medium were first centrifuged at 4000 rpm for 15 min to collect the supernatant, and then was filtered using a glass fiber filter (GC-50, 47mm; ADVANTEC, Japan). As for conditions with MQ water medium, the samples were taken directly without centrifugation and filtration. Then, all samples were diluted 1000 times in 3% of HNO_3 (Nitric acid, 60-61%; Wako, Japan) and filtered with a syringe filter (CA Syringe filters, 13mm, 0.45µm, Membrane Solutions, Japan) before analyzing it in the ICP machine.

4.3 Results and discussion

The results of Total Solids (TS) attachment on the sponges before and after plating are shown in Table 5. The result of the non-plated sponge condition shows that there are no significant differences on the biomass attachment on MS and PS, where MS is 0.0326 g-TS/sponge and PS is 0.0349 g-TS/sponge. However, both Ni-plated MS and PS exhibit lower biomass attachment compared to their non-plated counterparts. Specifically, biomass attachment on Ni-plated MS is approximately 1.15 times lower than on raw MS, and biomass attachment on Ni-plated PS is approximately 1.52 times lower than on raw PS. Studies have shown that rough surface materials with a large specific surface area can easily be colonized by microbes, achieving higher immobilization, which facilitates biofilm formations (Xiao et al., 2021). Hence, the reduced biomass attachment values observed after the plating of the sponges may be attributed to the deposition of nickel on the sponge surface, which could modify different factors; The porous volume of the MS sponges significantly decreased from 0.920 cm^3/cm^3 to 0.361 cm^3/cm^3 after nickel plating, and the porous volume of PS sponges slightly decreased from 1.429 cm^3/cm^3 to 1.424 cm^3/cm^3 (Table 6). The reduction in porosity suggests that many pores may be partially or fully blocked by the nickel plating. This blockage reduces the number of available sites for biomass to adhere within the sponge structure. The decreased porosity is directly related to a lower specific surface area, where carriers with higher porosity offer more internal surface area within the pores. Additionally, due to the uniform deposition of nickel on the sponge, the rugosity of the sponge surface is smoothed, and the internal surface of the sponge decreases, thus limiting the sites where microorganisms can adhere and grow. Besides, nickel deposition alters the surface properties of the sponges, potentially making them less favorable for microbial adhesion. For instance, the nickel-plated surfaces might become more hydrophobic, which generally discourages biomass attachment. Furthermore, the Ni-plated MS demonstrated a higher sludge attachment

capacity of 0.0275 g-TS/sponge compared to Ni-plated PS, which showed a capacity of 0.0169 g-TS/sponge, making the latter 1.63 times lower. This difference could be attributed to the higher surface area of MS compared to PS.

To evaluate the tightly bound biomass on the sponges, both MS and PS were washed with PBS solution post-experiment to remove the biomass that was not strongly adhered to their structure. Comparing these results to the condition without washing using PBS solution, the results show that MS can retain about 61.7% and PS could retain 27.0% of the attached biomass, respectively, after washing with the PBS solution. This result demonstrates that MS can immobilize and retain more biomass with approximately 3.7 times than PS, which could likely be attributed to the smaller pore size and higher surface area of the melamine sponge, which allows it to strongly retain the biofilm formed in their structures. Based on this result, the Ni-plated MS shows a promising result of adhering more biomass in AD which could contribute to an even more efficient DIET performance. However, after the 7-days experiment, some precipitation was observed in the MS MQ water as medium condition. After filtration, the precipitated particle appears to be the peeled off nickel from the sponge (Figure 13). In addition, 0.0038 g of MS particles were recovered post-filtration from the three sponges used in the trial, accounting for about 6.83% of nickel sponge mass peeled off from the entirety of the Ni-plated MS (Table 7). This is probably due to the poor durability of MS as concluded in chapter 2. These particles could be considered potential water pollutants, necessitating an additional step in the wastewater treatment process for their removal. Several countries have established their legislation setting limits on the parameters of treated wastewater effluent, including the concentration of nickel. For instance, in Spain, the Ni effluent concentration must be lower than 20 µg/L, including all the bioavailable concentrations of this substance, when the effluent is released into the environment (Boletín Oficial del Estado, 2015). Besides,

Chinese's national standards consider hazardous waste when the Ni concentration exceeds 0.5 mg/g (Ko et al., 2018). Therefore, the breakdown of nickel-plated sponge does not only threaten the environmental life cycle but also the optimum water quality after the AD process. In contrast, in the case of the Ni-plated PS in MQ water medium condition, no particles were found after filtration, suggesting that PS is highly resistant to detachment. The higher durability of PS not only reduces the potential of secondary Ni pollution but also indicates an extended life cycle, thereby enhancing its economic viability. Therefore, despite the high biomass adhesion of MS, PS will be used in the following continuous experiment to mitigate the risk of secondary heavy metal contamination.

Many research have highlighted that Ni is a crucial trace element for bacteria and archaea microbes and the addition of Ni^{2+} can increase the biogas production by 18% without affecting the pH during the AD process (Tian et al., 2016). Nevertheless, an excessive amount of Ni concentration reduces the AD process efficiency by causing the disintegration of microbial cell membranes (Kaur et al., 2021), and overloading with Ni^{2+} concentration in the reactor could inhibit the activity of hydrogen-producing bacteria (B. Zhao et al., 2022). Therefore, it is important to evaluate the Ni^{2+} releasing rate of the sponges to prevent inhibition in the subsequent AD experiment. Figure 14 shows the result of dissimilated Ni^{2+} concentration from the 3 Ni-plated sponges throughout the experiment in MQ water medium and in AD sludge. The results show that in MQ water medium, MS presents a slightly higher Ni^{2+} release compared to PS. This result is reasonable as there are more Ni deposited on MS compared to PS (Table 3), leading to higher Ni^{2+} released. The result also shows that the average Ni^{2+} releasing rate per day for MS and PS is 7.4 and 6.8 mg/L/day respectively. It has been reported that when the Ni^{2+} concentration is higher than 30 mg/L, Ni^{2+} could lead to an inhibitory effect on the

methanogenic activity; besides, higher concentrations of Ni^{2+} had stronger inhibition effects (Q. Guo et al., 2019). It should also be noted that these values were obtained at the stirring conditions at 170 rpm. Since the stirring could increase the releasing rate of Ni^{2+}, the releasing rate of Ni^{2+} could differ when using a UASB reactor. Therefore, future study on ion releasing rate of Ni-sponge should be carried out based on the design of reactor used for AD experiment. On the other hand, the result in Figure 14 also shows that when nickel-plated sponge is inoculated inside the AD sludge medium, the concentration of released Ni^{2+} is way lower than when inoculated in the MQ water medium. It has been reported that anaerobic sludge has the capacity to absorb metal ions such as Ni^{2+} (Haytogiu et al., 2001). Since the pretreatment was conducted prior to the ICP measurement for the conditions inoculated in AD sludge, where biomass was removed by centrifugation and filtration, the lower Ni^{2+} concentration in AD sludge inoculum is reasonable. Interestingly, the result of Ni^{2+} concentration for PS condition is higher than in MS condition, which differs from the result when inoculated in MQ water medium. As mentioned above, one of the possible reasons may be due to the biomass attachment on the sponge, which could absorb the metal ion. Another possible reason could be the biomass attachment on the sponge creating a physical barrier, thereby reducing the release of nickel ion. Based on the biomass attachment result in Table 5, MS sponge exhibits not only higher biomass attachment values (1.62 times) but also a tighter bound biomass (3.7 times) than PS. Thereby, the result of lower Ni^{2+} concentration in MS condition could be due to more biomass attachment compared to PS. Furthermore, as mentioned before, Ni is an elemental trace element that can be used by AD microbes during their metabolism (Moestedt et al., 2016b). Although it is unlikely that most Ni is consumed by the microbes, there is also a possibility where little concentration of Ni was consumed by the microbes. Since microbes' attachment on the sponge is known to

enhance their metabolism, this could lead to higher Ni consumption by the microbes retained in MS, contributing to the result in Figure 14.

These Ni^{2+} ICP results indicate the tendency of each sponge to release Ni^{2+} during the process. However, since the UASB reactor does not exert a mechanical breakdown potential on the sponges as high as that of the stirrer used for this experiment, these results will not be considered for determining the amount of sponges used in the UASB continuous experiment.

Table 5. Total solids attached on each sponge condition after 7-days of experiment

Plated/Non plated	Sponge	Medium	Biomass attached to the sponge (g)
Non-Plated	MS	Sludge	0.0326
	PS		0.0349
Plated	MS	Water	-0.0041
		Sludge	0.0275
		Tightly bound biomass	0.017
	PS	Water	-0.0002
		Sludge	0.0169
		Tightly bound biomass	0.0046

Table 6. Sponges' pores volume

	Pores volume (cm3/cm3 of sponge)	
	MS	PS
Raw	0.920	1.429
Plated	0.361	1.424

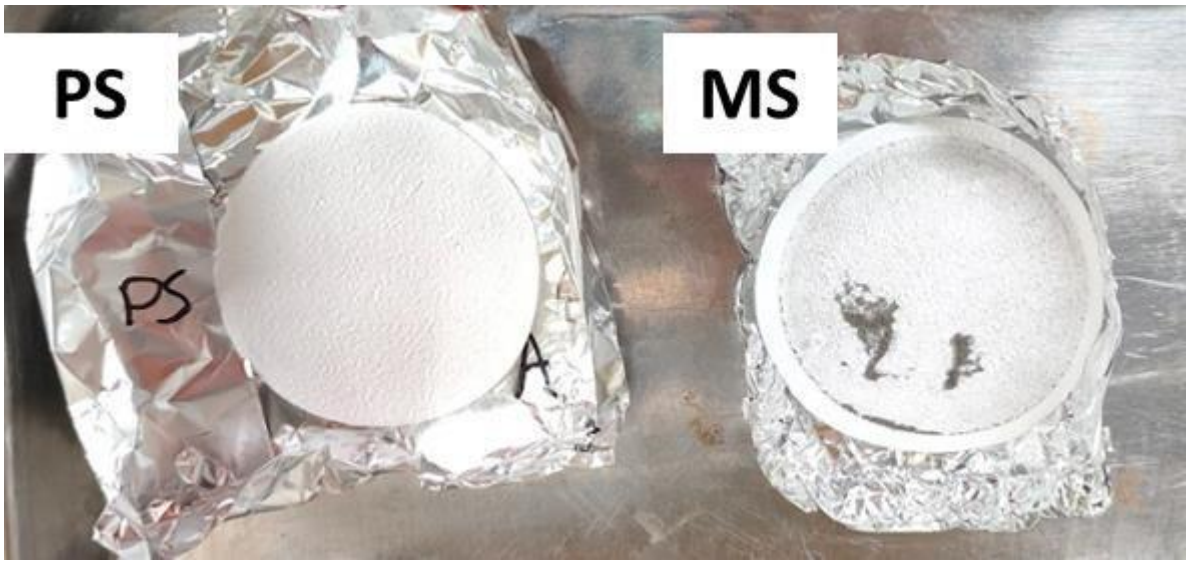

Figure 13. Precipitation found in Ni-plated polyurethane sponge and melamine sponge in MQ water medium after 7-days experiment

Table 7. Weight of Ni peeled off from Ni-plated melamine sponge and polyurethane sponge after 7-days experiment

Sponge	Total sponge used (g)	Particle weight (g)	% Sponge peeled-off
MS	0.0556	0.0038	6.83%
PS	0.1726	0.0000	0.00%

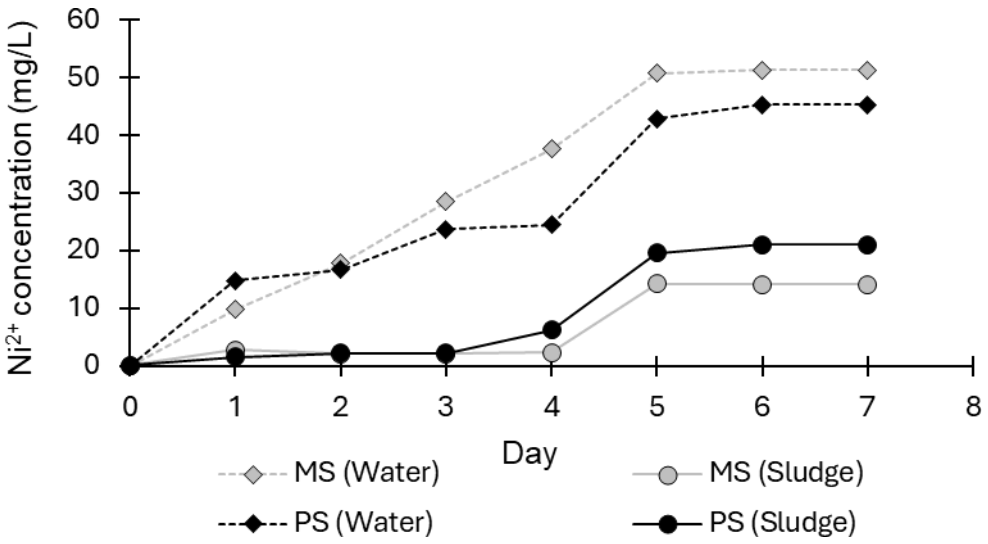

Figure 14. Cumulative released Ni^{2+} concentration from Ni-plated melamine sponge and polyurethane sponge in each medium throughout the 7-day experiment

4.4 Conclusion

The experimental results demonstrate significant differences between MS and PS sponges in terms of biomass attachment and nickel release. While Ni-plated MS exhibits higher biomass attachment and tighter bound biomass, it also shows a higher propensity for nickel to be peeled off the sponge. These could pose a risk of secondary heavy metal contamination, necessitating additional water treatment steps, and suggesting a shorter life cycle for MS compared to PS. The Ni^{2+} release rate from MS also shows a higher concentration compared to PS due to the higher nickel deposition on the MS. This may also hinder the microbes' activity when attached to the MS which has such high concentration. Therefore, despite the MS exhibiting higher biomass adhesion, PS will be used in the subsequent continuous experiment to mitigate the risk of secondary contamination and prevent higher chances of inhibiting microbes’ activity.

Chapter 5: Evaluation of the anaerobic digestion continuous experiment performance with the addition of Ni-electroless plated sponges in UASB reactor.

5.1 Background/Overview of Experiment 4.

In chapter 4, it was observed that the nickel plating on the melamine sponge (Ni-MS) exhibited some degree of peeling at the end of the experiment. Conversely, no detachment of nickel plating was observed when using the nickel-plated polyurethane sponge (Ni-PS). Therefore, it is concluded that Ni-PS is the more suitable material for application in the AD process. This is due to its potential to mitigate secondary heavy pollution and its suitability for long-term experimental use. Thereby, in this chapter, addition of Ni-PS to UASB reactor will be attempted, and its methane production efficiency will be evaluated.

In this study, evaluation of Ni-PS applied in AD process will be conducted and compared to the condition without any addition of Ni-PS, which will serve as control. This comparison aims to assess the overall performance of the AD performance. As hypothesis, condition with the addition of Ni-PS will achieve a higher methane production and TOC removal rate as compared to control.

5.2 Methods and materials

5.2.1 Sponges plating

The electroless Ni-plating method described in Chapter 3, section 3.2.2 was applied in this experiment. However, it should be noted that the plating method describe in chapter 3 was conducted on a small scale. Therefore, the only modification made in this study was the use of a larger volume of solution, scaled up in proportion to the number of sponges being plated simultaneously. This adjustment was made to ensure that all sponges are plated efficiently and evenly together. Another modification made in this study was that the sponges were not placed in a net for subsequent soaking; but were directly placed in the beaker and soaked in the respective solution while being gently stirred with chopsticks.

In this study, a total of 350 mL volume of polyurethane sponge was plated. After plating, the sponge's weight increase and conductivity were evaluated. Before inoculating the plated sponge into the AD system, the sponges were pretreated to remove any potential impurities which could inhibit the AD system. The pretreatment method was based on (Li et al., 2021), in brief, the sponges were soaked in ethanol for 10 mins and continued by washing in an ultrasonic bath for another 10 mins. This process was repeated three times. Finally, the sponges were dried again at 80ºC for 2.5 hours before being added to the AD system.

5.2.2 Experiment set-up

5.2.2.1 Preculturing conditions

To achieve a higher efficiency in the UASB reactor, a preculture period was made for microbes to be immobilized on the Ni-PS. The preculturing was set up in a batch operation, where in brief two 1 L of medium glass bottle was prepared for the following conditions: 1) 700 mL of AD sludge as "control" and 2) 600 mL of AD sludge with the

addition of 350 mL volume of Ni-PS as “Nickel addition”. The sludge used was obtained from the Hakubu Sludge Treatment Centre (Yokohama, Japan). For this preculture, ethanol was used as substrate with an inoculum-to-substrate ratio of 2:1 VS- base. Table XA) shows the TS and VS contents in the inoculated sludge where VS value is 17.38 g-VS/L. The preculture was carried out for 20 days in a thermal bath at 37ºC and stirred at 100 rpm, using a stirring motor. After 20 days, the TS and VS of the two conditions were measured again to ensure if there were any significant difference. The pH of both conditions was adjusted to pH 7.7 using HCl and NaOH, before transferring the precultured-sludge into the UASB reactor, as will be described in the next section.

5.2.2.2 UASB reactor set-up

Two lab-scale UASB reactor, each with an effective working volume of 1.2 L were used in this study. The first reactor was operated as “control” without any additional material, while the second reactor was supplemented with Ni-PS sponge. These conditions were chosen to compare the wastewater treatment performance by the conventional AD UASB reactor operation with the addition of Ni-PS carrier as a conductive material. Both conditions were adjusted to the same inoculated VS concentration at the beginning of the experiment, with trial 1 showing a concentration of 11.76g/L (Table 8), and trial 2 having 17.83 g/L (Table 9). At the beginning of the experiment, a 1:1 ratio of AD sludge and substrate was inoculated into the UASB reactor, resulting in each reactor receiving 600 mL of AD sludge and 600 mL of substrate, which was then left to settle for 3 days. The substrate (ethanol) was added at the sludge to substrate ratio of 2:1 (VS-based) and diluted until the total volume reached 600 mL. This step is to allow the sludge to acclimate while settling before introducing the influent.

After 3 days of sludge settling, the reactors were supplied with synthetic brewery wastewater based on (Zhao et al, 2015). The composition of this synthetic wastewater per

liter is as follows: 2.35 mL of ethanol, 0.2162 g of KH_2PO_4, 0.1034 g of K_2HPO_4, 0.1598 g of Na_2SO_4, 0.047 g of $MgCl_2.6H_2O$, 0.094 g of $CaCl_2.2H_2O$, 9.4 mL of trace element and 9.4 mL of vitamin solution. The trace element and vitamin solution was based on (Morita et al., 2011) and its composition is listed in Table 10. The primary carbon source in this synthetic wastewater was ethanol, contributing approximately 3.875 g-COD/L. Prior to introduction into the reactors, the pH of the substrate was adjusted to about 7.3 with sodium hydroxide, followed by deoxygenation through nitrogen gas flushing for about one hour. The synthetic wastewater was then pumped into the reactor using a peristaltic pump. The initial hydraulic retention time (HRT) was set to 7 days to achieve an OLR of 0.5 g-COD/L/d. From day 9 onwards, the HRT was shortened to 9 days to reach an OLR of 0.42 g-COD/L/d due to rapid acidification observed in the reactor. The influent and effluent were kept under 4℃. Before starting the experiment, the dead space of the UASB reactor was purged with nitrogen gas for 2 mins to achieve an anaerobic condition. A gas bag was then attached to the top of the reactor to collect the produced biogas. Sampling for biogas production, influent, effluent was conducted 3 times a week, along with measurements of the pH of both influent and effluent. Additionally, 15 mL of sludge was taken from the sample port daily to measure the pH inside the reactor; the sludge was then returned into the reactor to maintain a consistent sludge volume throughout the experiment. To prevent acidification and ensure stable conditions, the pH of the inoculum was adjusted with NaOH or $Ca(OH)_2$ whenever it dropped below 6.8. It should note that on the sampling days, all reactors were purged with 100 mL of nitrogen gas from the bottom to disintegrate large floating sludge particles and ensure substrate homogeneity at the initial stage.

Table 8. Trial 1 sludge TS-VS concentration

Condition	TS avergae (g-TS/g sample)	VS average (g-VS/g sample)
Before preculture		
Sludge	21.02	17.38
After preculture		
Nickel addition	20.58	11.82
Control	19.47	12.68

Table 9. Trial 2 sludge TS-VS concentration

Condition	TS avergae (g-TS/g sample)	VS average (g-VS/g sample)
Sludge	22.82	17.83

Table 10. Component of Trace Element and Vitamin Solution

Trace element solution	
Component	**Concentration (g L-1)**
$MnSO_4 \cdot H_2O$	0.5
$FeSO_4 \cdot 7H_2O$	0.1
$NiCl_2 \cdot 6H2O$	0.04
$CoCl_2 \cdot 6H_2O$	0.05
$ZnCl_2$	0.13
$CuSO_4 \cdot 5H_2O$	0.01
$AlK(SO_4)_2 \cdot 12H_2O$	0.01
H_3BO_3	0.01
$Na_2MoO_4 \cdot 2H_2O$	0.025
Vitamin Solution	
Biotin	0.002
Pantothenic acid	0.005
B-12	0.0001
ρ-aminobenzoic acid	0.005
Thioctic acid	0.005
Nicotinic acid	0.005
Riboflavin	0.005
Pyridosine HCl	0.01
Folic acid	0.002

5.2.3 Analytic methods

Total Solids (TS) and Volatile Solids (VS) were measured before the experiment using the methods from the American Public Health Association (American Public Health Association, 2005). The volume of the biogas was measured manually using a 500 ml syring connected to the gas bag. As for the biogas composition, it was analyzsed by the gas chromatograph with thermal conductivity detector (TCD) (Shimadzu Gas Chromatography, GC-2014) equipped with Active Carbon packed column. The injector, detector and column temperatures were maintained at 120 ℃ , 120 ℃ and 100 ℃ respectively. The detector current was set to 65 mA, while argon was used as carrier gas with a flow rate of 40 mL min^{-1}.

For the effluent samples were filtered using a glass fiber filter (GC-50, 47mm; ADVANTEC, Japan) and stored together with influent samples at below -20℃ until further analysis. The VFA (precisely only acetate) and ethanol were analyzed using gas chromatography with a flame ionization detector (FID) (Shimadzu Gas Chromatography, GC-2014) equipped with a BX-100 60/80 glass column and a Unisole F-200 30/60 glass column. For analyzing ethanol, the injector, detector, and column temperatures were maintained at 250°C, 110°C, and 110°C, respectively, with nitrogen used as the carrier gas at a flow rate of 32 mL min^{-1}. For analyzing VFAs, the injector, detector, and column temperatures were maintained at 200°C, 140°C, and 140°C, with nitrogen used as the carrier gas at a flow rate of 35 mL min^{-1}. pH was measured using a pH meter (Bettler Toledo, S220-Basic). The Total Organic Carbon (TOC) was analysed by TOC analyser (Shimadzu, TOC-L CPH/CPN). Finally, Nickel and other methal concentration in the filtered liquid sample was measured by an inductively coupled plasma Inductively Coupled Plasma machine (7850, ICP-MS, Agilent, Japan). For this measurement, a sample of the sludge was taken before start the experiment and after 39 days of the

experiment, another sample was taken from the sampling tube of the UASB reactor of both conditions. The sludge samples were centrifuged at 4000 rpm for 15 min to collect the supernatant, and then was filtered using a glass fiber filter (GC-50, 47mm; ADVANTEC, Japan) and stored at below -20℃ until further analysis.

5.2.4 Theorical methane production

To ensure that all the methane produced in the AD process is recovered in the biogas bags, the theorical methane production is calculated by comparing the total daily Chemical Organic Demand (COD) in the influent and effluent using equation 6.

$$TMP = (\mathrm{CODin} - \mathrm{CODeff}) \times 350\mathrm{mL}\left(\frac{\mathrm{CH4}}{\mathrm{g\ COD}}\right) \quad \text{(Eq.6)}$$

Where TMP is the Theorical methane production, CODin is the total COD per day in the influent and CODeff is the total COD per day in the effluent.

5.2.5 Methanogenesis efficiency

To evaluate the performance of the conversion of acetate into biogas by methanogens, the methanogenesis efficiency during the AD process was calculated by the equation 7,

$$Me = \frac{Mp}{(Mp+A)} \times 100\% \quad \text{(Eq.7)}$$

Where Me is the methanogenesis efficiency, Mp is the daily methane production (g-COD), and A is the acetate in the effluent (g-COD). It should be noted that in this experiment, the COD of methane and acetate was calculated theoretically from the produced cumulative methane production and initial ethanol concentration analyzed from GC-FID where 1mL-CH_4 = 2.857 g-COD, while 1 g-acetate = 1.085 g-COD.

5.3 Results and discussion

5.3.1 First trial of the Experiment

Before evaluating the Ni-PS in the continuous UASB experiment, a pre-culturing period was conducted to allow microbes to acclimate and immobilize onto the Ni-PS enhancing performance when transferred to the UASB reactor. It should be noted that due to the leakage from the reactor, biogas could not be measured throughout the pre-culturing period. However, pH was monitored periodically to ensure the AD process remained within a suitable pH range.

On day 9 of the pre-culture, a layer of scum-like debris was observed on the surface of the Ni addition condition (Figure 15). Suspecting that low agitation in the reactor might have caused the scum formation, the scum was removed, and pre-culturing continued until day 20. It should be noted that most of the "scum" formed on the surface of the floating sponge, so complete removal was not possible.

After the pre-culturing period the sludge and sponges were transferred to the UASB reactor for sludge settling. During this period, substrate was also inoculated without introducing the influent to prevent microbial starvation. However, even after 4 days of settling, white solid spots that look like mold were found on top of the reactor in the Ni-PS added condition (Figure 16). Additionally, the pH remained constant throughout the settling period (7.80) and only about 120 mL of biogas was produced throughout the 4 days. In contrast, the control condition's pH shifted from 7.7 to 7.49 by day 4, with a total biogas production of about 720 mL, six times more than the Ni-PS added condition (result not shown).

Based on these results, contamination might have occurred in the Ni-PS added condition reactor, causing the AD process to stop. For the next trial, the sponges were

thoroughly washed using the Li et al., 2021, method, before being introduced into the AD system to prevent any possible contamination. Another possible reason for the AD system's failure in this trial was the overload of nickel concentration. Studies have shown that a high concentration of Ni^{2+} can cause microbial cell membranes to disintegrate. Since the pre-culturing was carried out with a stirring motor, the Ni^{2+} release rate might have increased and accumulated in the batch system, inhibiting the AD process. Therefore, in the next trial, a lesser amount of Ni-PS will be used (10% of the total UASB reactor's volume) without any pre-culturing due to time constraints and the potential accumulation of Ni^{2+} in the reactor.

Figure 15. Experiment 4 trial 1 contamination

Figure 16. Experiment 4 trial 1 UASB reactor contamination

5.3.2 Second trial of the Experiment

In the second trial experiment, Ni-PS was added after the sludge had settled in the UASB reactor. However, after the addition of Ni-PS, sponge floatation was observed throughout the experiment (Figure 17). As mentioned in the introduction, the DIET mechanism can only occur when DIET-related microbes are attached to conductive materials. In this case, the floatation of the sponge was separated from the settled biomass, preventing the DIET mechanism from occurring. Attempts were made to settle the sponges by opening the UASB reactor and stirring from the above. Although the sponges were settled after stirring them, floatation was observed again the next day. Therefore, to submerge the sponge towards the bottom of the reactor, a net was introduced from day 9 onwards (Figure 18). The net was handmade using non-conductive materials to ensure it would not affect the AD process through the DIET mechanism.

It is important to note that, during the first 9 days, a technical issue with influent pump caused inconsistent influent flow between the two conditions. Additionally, the pH of both reactors decreased over time (Figure 19-A). Although the pH remained within the range for AD to proceed, the OLR was re-adjusted to 0.42 g-COD/L/d from day 9 onwards to prevent further acidification in the reactor. From day 9 onwards, the flow rate for both reactors was fixed to the same rate. Thereby, the results discussion will focus on the period from day 9 onwards.

Figure 20-A shows the concentration of ethanol for influent and effluent, while Figure 20-B shows the concentration of acetate in the effluent for both conditions. The results indicate that all ethanol was consumed, as no ethanol was detected in the effluent, suggesting high activity of acetogenic bacteria in both conditions. In contrast, the nickel addition condition exhibited a slightly lower acetate concentration in the effluent than in the control condition. These findings suggest that the addition of Ni-PS may accelerate

the methanogenesis process due to the following two reasons. First, previous studies have shown that adding nickel to AD system can enhance methanogenic activity, as methanogenesis is an enzymatic pathway with high dependency on metal ions (Hijazi et al., 2020). Specifically, Ni^{2+} is the central ion in coenzyme of methyl-CoM to CH_4 in the methanogenesis process (Glass & Orphan, 2012). Therefore, the addition of Ni-PS could have increased methanogenic activity. Second, the addition of Ni-PS may have facilitated DIET, acting as a bridge for electron transfer between exoelectrogenic bacteria and methanogens. However, further studies such as the microbial community to check the presence of DIET participating exoelectrogenic bacteria and methanogens and DIET functional genes must be analyzed to confirm the occurrence of DIET mechanism in the Ni-addition condition.

Figure 21 shows the result of daily biogas and methane gas production for both conditions. From day 9, both biogas and methane production were consistently higher in the control condition than in the Ni-added condition throughout the experiment. The result indicates that the average methane production in the control condition was 1.64 times higher than in the Ni-added condition. However, the total organic loading (TOC) removal rates (Figure 22) were similar for both conditions, with over 95% TOC removed observed. It should be noted that, to prevent the sludge from settling down on the net after purging N_2 gas from the bottom of the UASB reactor, the net was removed every two days. Upon removing the net, a large amount of gas bubbles was observed, accompanied by the floatation of sponge along with a layer of sludge surrounding it. Therefore, the lower methane production in the nickel-added condition is possibly due to the formation of a sludge layer on the sponge surface, which traps the biogas and prevents its release and recovery into the gas bags. To verify the above statement, the theorical methane production of both conditions (Figure 23-A) was calculated based on the acetate

consumed by methanogens during the AD process. Results shown a slightly higher theorical methane production in the Ni-PS condition until day 25. Additionally, the methanogens activity in both reactors was calculated based on the percentage (%) of acetate converted to methane (Figure 23-B). The results indicated a slightly higher efficiency in the Ni-PS condition compared to the control condition between the day 11-25, achieving an increase of 9% on day 17. This results indicate that the addition of Ni-PS could help the process to stabilize faster. The faster acetate consumption not only can enhance the methane production but also may allow the reactor to perform under higher OLR's avoiding the accumulation of acetate and consequently the acidification of the reactor.

As shown above, Figure 19 shows the result of pH in both reactor and effluent for the two conditions. The results indicate that the Ni-added condition had a slightly higher pH compared to the control. This observation correlates with effluent acetate concentration results. Although the pH in the reactor is relatively low, it is still at the range for AD process to proceed. Besides, the influent pH remained lower than the effluent pH on most days (Figure 19-B), indicating that AD was still progressing. Overall, this study demonstrates that the addition of Ni-PS to the AD system can enhance performance. However, further research is needed to improve biogas permeability, ensuring that all produced biogas is efficiently captured.

Figure 24 shows the ICP results. The Ni^{2+} concentration in the sludge before and after the experiment is shown in the Figure 24-A, where the control condition did not show Ni^{2+} in the sludge after the experiment, which suggest that the UASB reactor operation removes Ni^{2+} over the course of the experiment. On the other hand, in the Ni-PS condition the Ni^{2+} concentration after the experiment was lower than before the experiment, which suggests that the addition of Ni-PS did not contribute to releasing Ni^{2+}

contaminants over the initial concentration in the sludge. Additionally, the Ni^{2+} concentration in the Ni-PS condition's effluent is represented in Figure 24-B. Early measurements showed concentrations over the initial concentration of the sludge (1500 mg/L) due to the sponges leaching before the net addition during the sludge's settling period. This concentration decreased to around 1000 mg/L by day 7, indicating initial leaching from the sludge. From day 7 to day 30, Ni^{2+} levels fluctuated between 0 and 1500 mg/L, reflecting dynamic equilibrium influenced by biological activity and reactor operation. After day 30, Ni^{2+} concentrations steadily declined, dropping below 500 mg/L by day 30 and remaining low until day 36, indicating stabilization. These results suggest that UASB reactors initially experience significant Ni^{2+} leaching, followed by a period of stabilization where effluent Ni^{2+} levels decrease substantially while the Ni-PS does not release higher Ni^{2+} concentrations than the initial sludge. This highlights the reactors' potential for managing heavy metal concentrations over time in wastewater treatment.

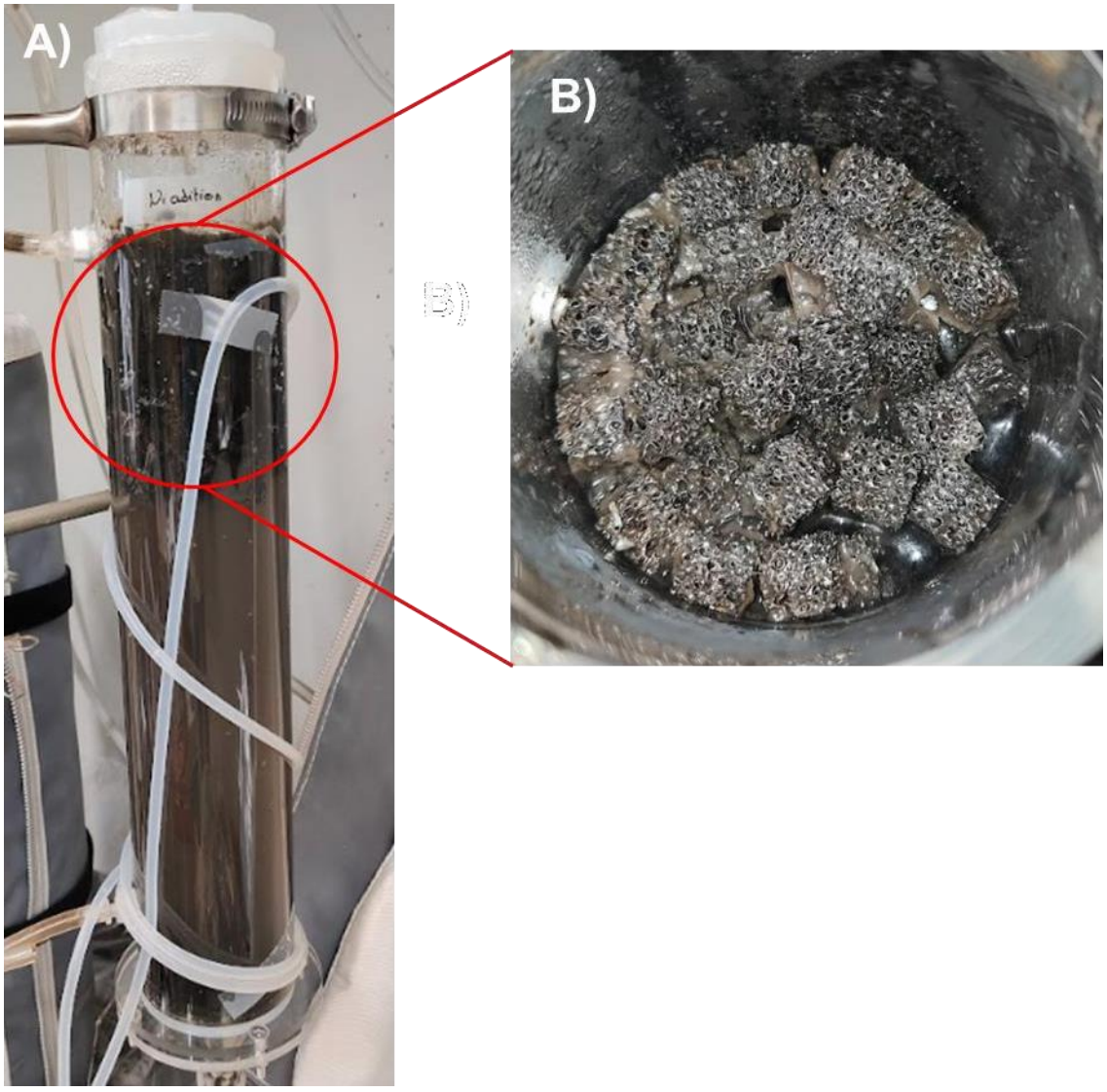

Figure 17. Experiment 4 trial 2 (A and B) sponges floating in the reactor

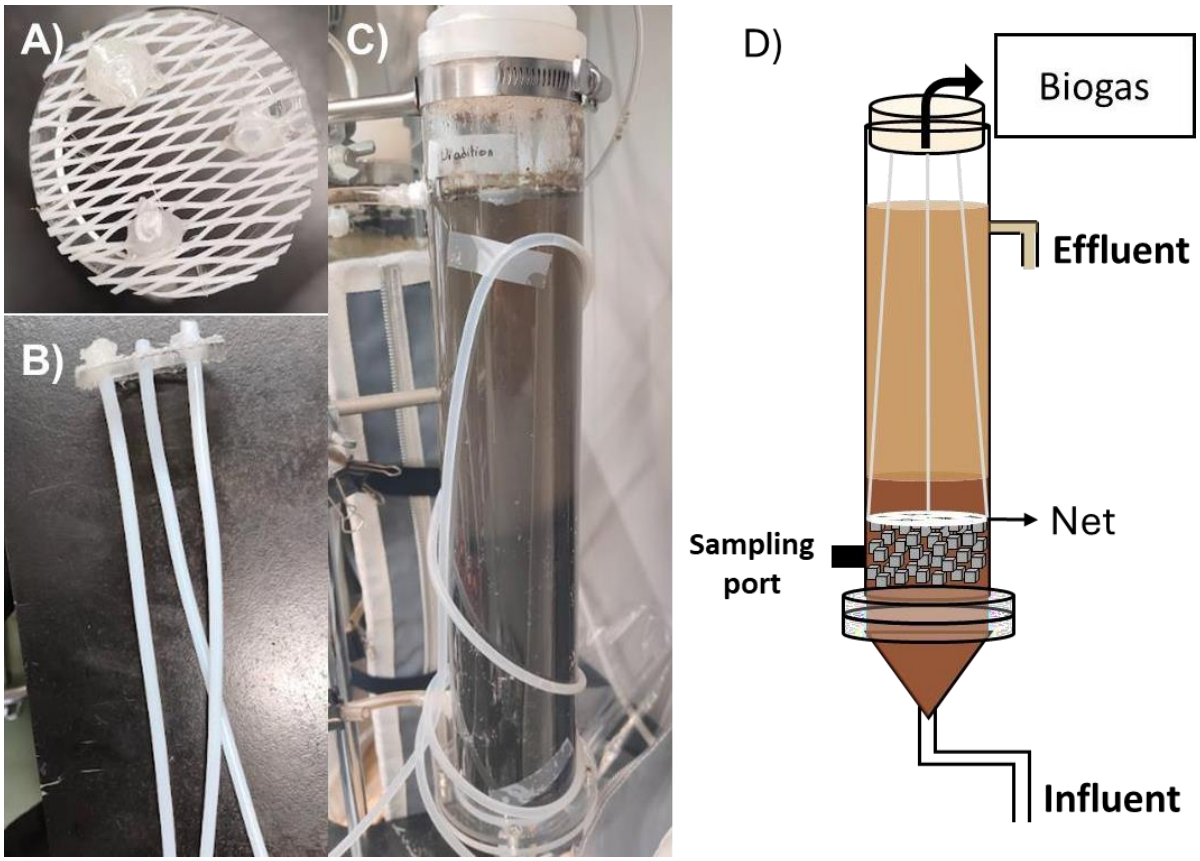

Figure 18. (A and B) Net used during the experiment (C) Net installed in the reactor (D) Scheme of the installed net

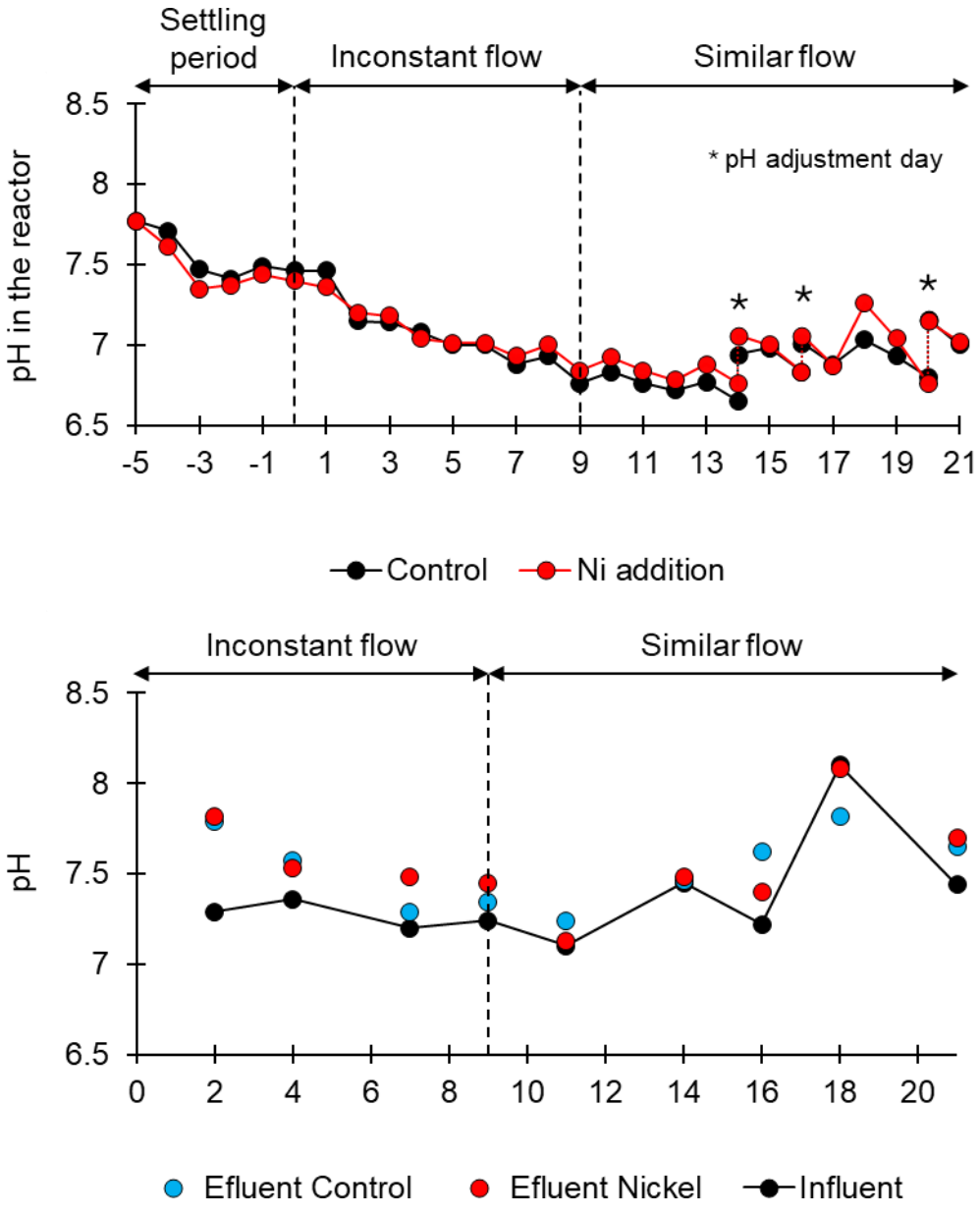

Figure 19. (A) pH in the reactor (B) effluent and influent pH

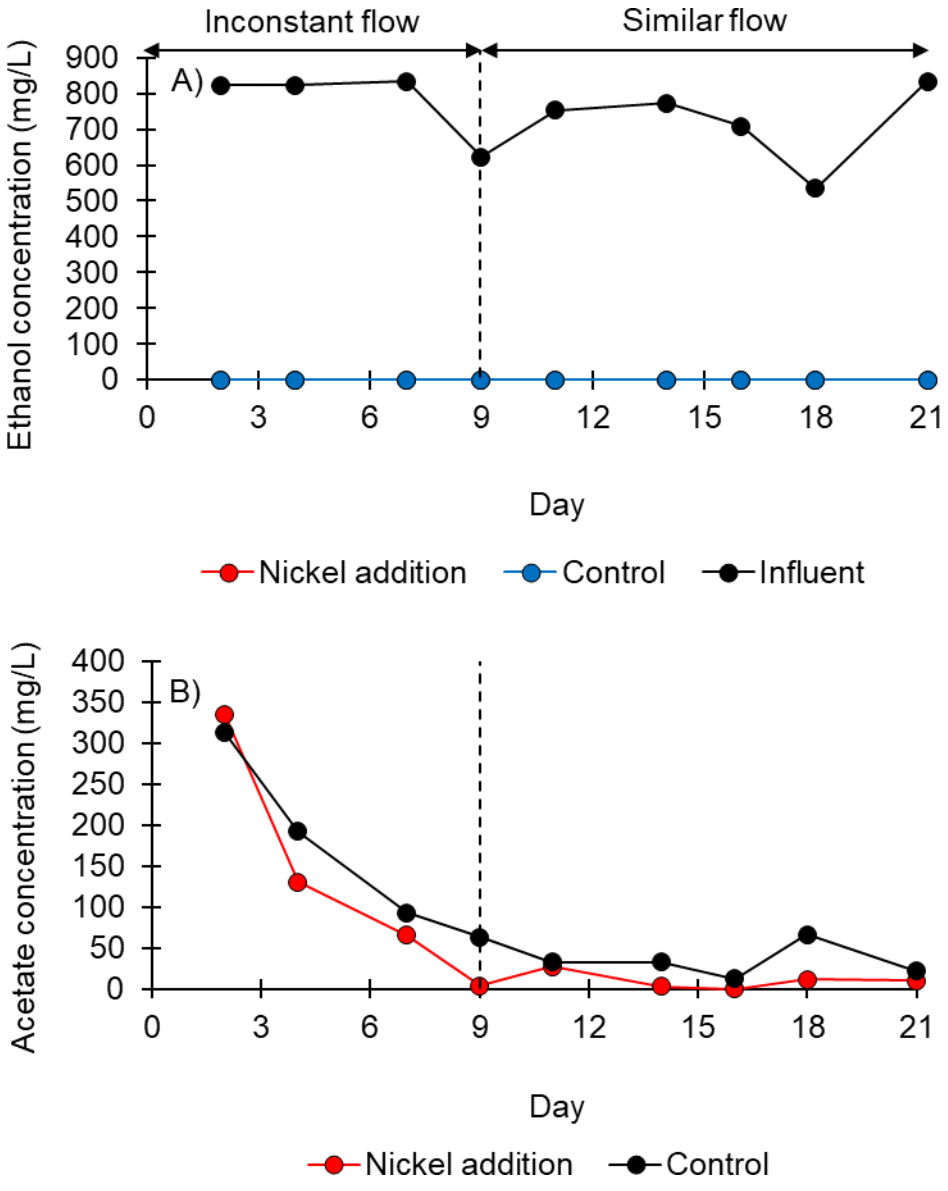

Figure 20. (A) Ethanol concentration (B) Acetate concentration

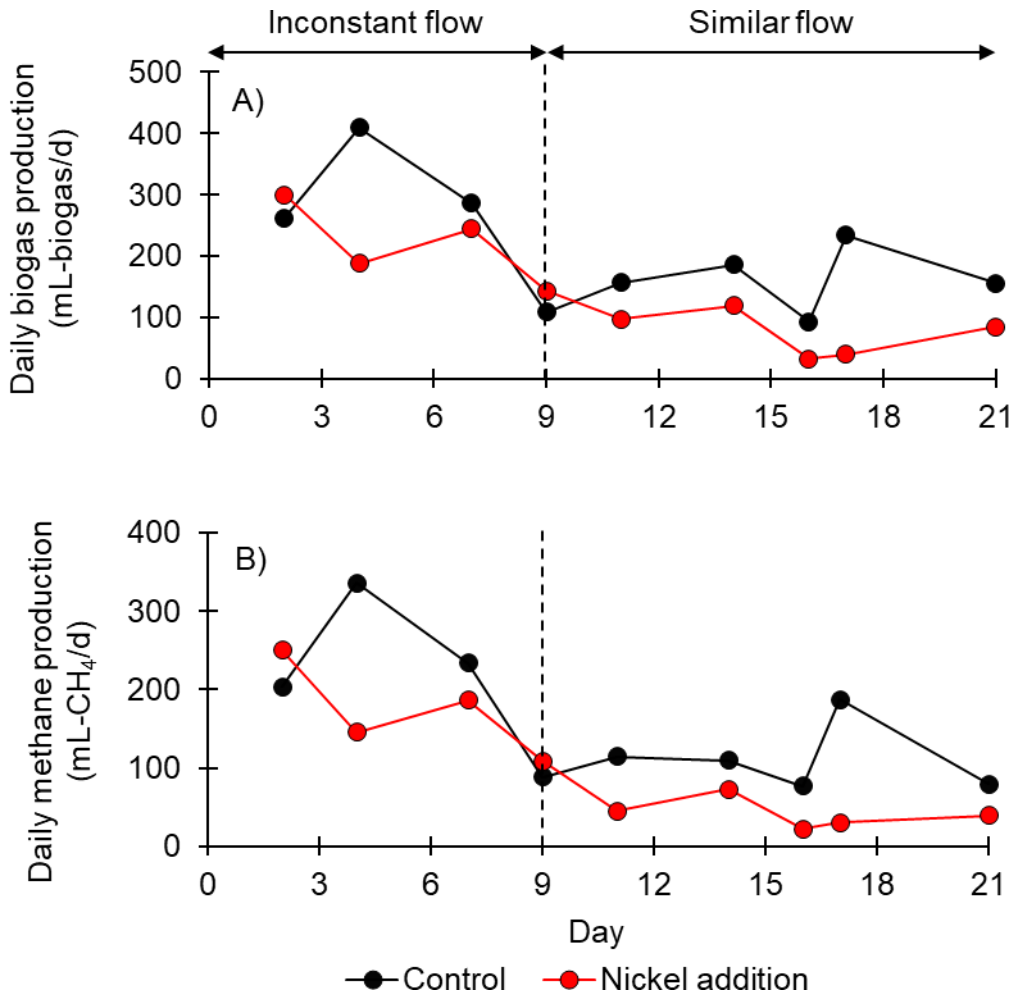

Figure 21. (A) Daily biogas production (B) daily methane production.

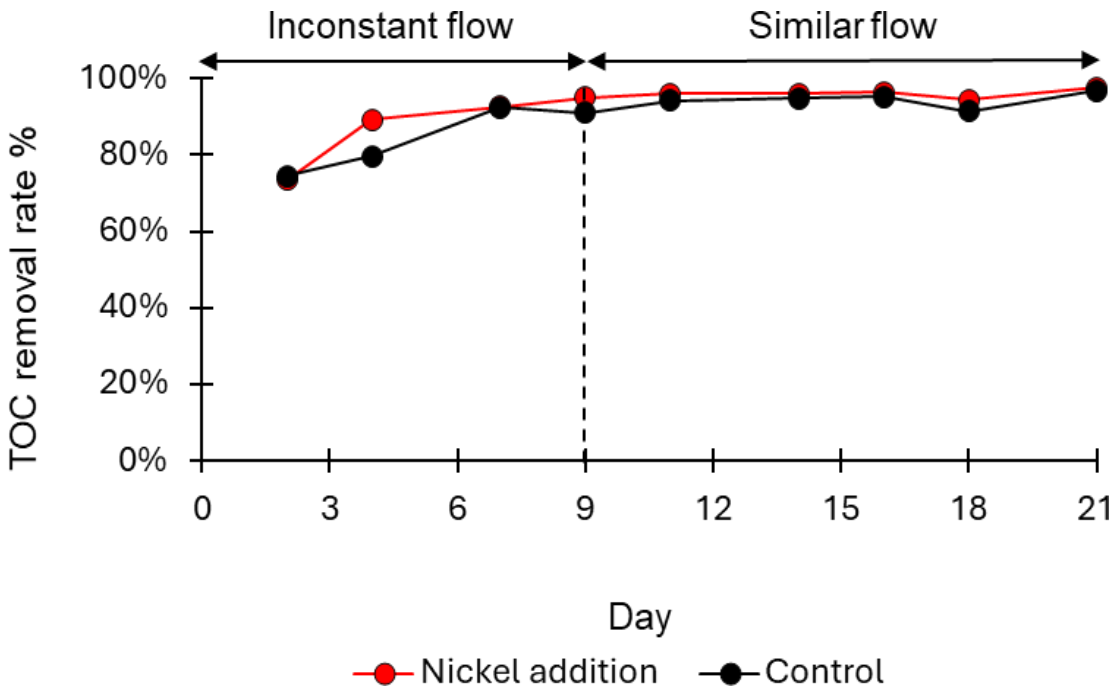

Figure 22. TOC removal rate

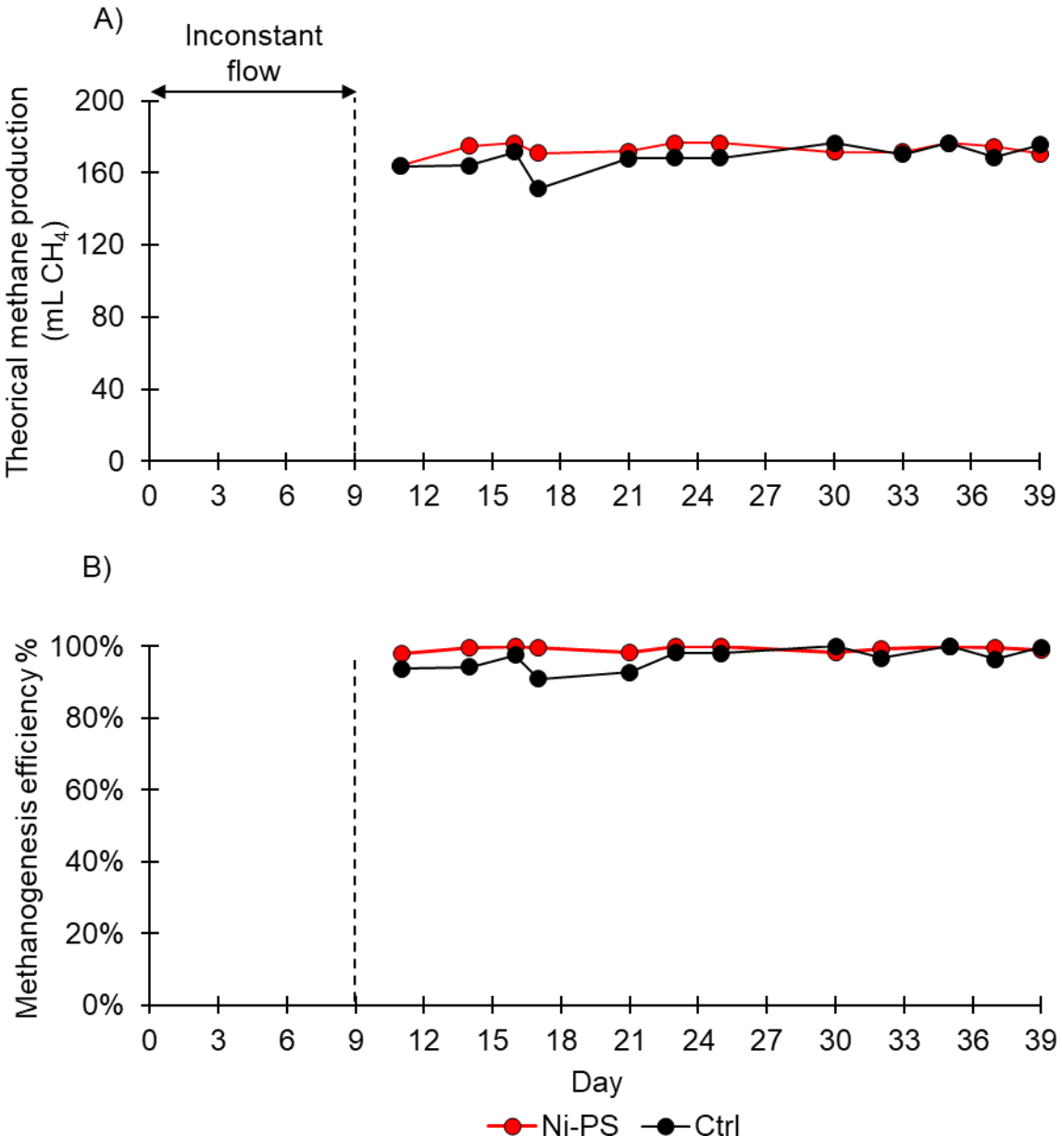

Figure 23. (A) Theorical methane production (B) Methanogenesis efficiency %

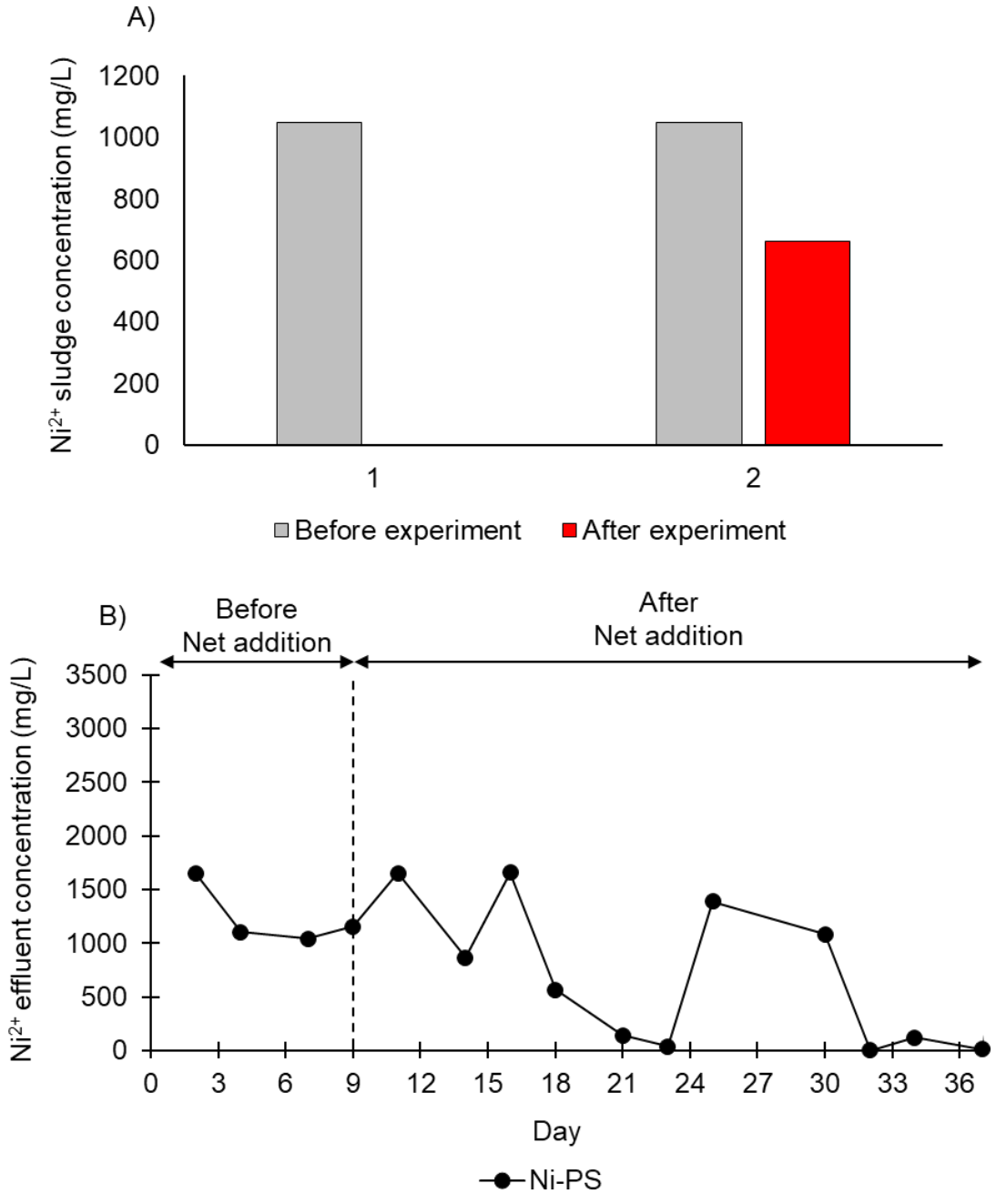

Figure 24. (A) Ni^{2+} concentration in the sludge (B) Ni^{2+} effluent's concentration in the Ni-PS condition.

5.4 Conclusion

In this chapter, nickel plated polyurethane sponge (Ni-PS) was applied into the UASB reactor, with the aim of enhancing the anaerobic digestion performance through the DIET mechanism. The results show that the Ni-PS condition also demonstrated lower volatile fatty acid (VFA) concentrations, indicating more efficient acetate metabolism by methanogens. These results suggest that the addition of Ni-PS sponges may enhance the anaerobic digestion process's efficiency and manageability. However, the entrapment of biogas in the Ni-PS reactor due to the biomass layer on the sponges, made it difficult to capture all the produced biogas. The entrapment of biogas in the reactor may also affect the AD process in the reactor leading to the decrease in pH. Therefore, these issues have to be addressed in future studies. Overall, despite the challenges in biogas recovery and the pH stability, the application of Ni-PS sponges in the UASB reactor improved removal rate of organic matter stability and effluent quality, suggesting their beneficial impact on optimizing anaerobic digestion performance.

Chapter 6: Conclusion & future perspective

In this study, the trial of applying nickel plated sponge via electroless plating method in the AD system to enhance the contact efficiency between microbes for a better performance on the DIET (Direct Interspecies Electron Transfer) was conducted. Four different experiments have been made to extend the application of nickel-plated sponge into the AD system by:

1. Evaluating Melamine Sponge's biotoxicity in anaerobic digestion process.
2. Trial in plating nickel on polyurethane sponge and melamine sponge via electroless plating method.
3. Evaluating nickel plated melamine sponge and polyurethane sponge for selection as immobilizations carrier for anaerobic digestion experiment.
4. Evaluating continuous anaerobic digestion performance with the addition of nickel-plated sponges in UASB reactor.

In chapter 2, the performance of melamine sponges (MS) in the anaerobic digestion (AD) batch process was evaluated. The results showed that MS does not have any biotoxic effects on microbial metabolism. The addition of MS increased methane production and shortened the lag phase compared to the control. However, MS was unsuitable for use in stirring reactors due to its poor durability, leading to sponge breakdown through friction. Nonetheless, MS maintained its integrity in the UASB reactor for 17 days, suggesting that future studies should utilize the UASB reactor.

In chapter 3, the electroless nickel plating method on polyurethane (PS) and melamine sponges (MS) was performed to assess their plating suitability. The results indicated that nickel plating was successful on both PS and MS, with MS showing higher nickel deposition likely due to its larger surface area. Both sponges exhibited conductivity throughout, confirming effective plating. Thereby, both plated sponges were further

analyzed in the next chapter to determine which plated sponge was more suitable to be applied in the AD experiment.

In chapter 4, the biomass attachment and nickel ion release rate of Ni-MS and Ni-PS were evaluated. Ni-MS had higher biomass attachment and tighter bound biomass compared to Ni-PS. Nevertheless, precipitation of peeled off nickel was found in the Ni-MS condition, which could lead to the risk of heavy metal contamination and requiring additional water treatment. Further, the Ni-MS had a higher Ni^{2+} release rate compared to Ni-PS, which could potentially disrupt microbial activity if not adjusted well. Thus, despite Ni-MS's higher biomass adhesion, Ni-PS will be used in continuous experiments to reduce the risk of contamination and avoid inhibiting microbial activity.

In chapter 5, the addition of Ni-PS showed a lower VFA concentration in the effluent compared to the control condition. This result suggests that the addition of Ni-PS to the AD system could accelerate the methanogenesis activity compared to the non-added condition. Based on the lower VFA concentrations compared to the control, possible higher methane production should be observed. However, throughout the study, the condition with added Ni-PS shows a significantly lower biogas production compared to the control condition. The lower biogas production may be due to the trapped biogas in the sponge/sludge layer. Despite challenges related to biogas recovery, the application of nickel-plated polyurethane sponges via electroless method in the anaerobic digestion system has demonstrated potential to enhance organic matter removal and effluent quality, highlighting their ability to optimize the performance of the anaerobic digestion process within a short 1-month study.

In the future, more studies should be conducted before applying it to practical use. In this study, floatation of sponge, along with the entrapment of biogas, was observed. Although the floatation issue can be easily overcome by introducing a net into the UASB

system to prevent washout, the biogas entrapped inside the sponge could not be efficiently captured. Additionally, the entrapment of biogas withing the sponge limits the diffusion of substrates into the sponge, leading to an inefficient process. Thus, optimization of the nickel-plated polyurethane sponge is necessary for future studies. It was also observed that the methanogenesis activity in the Ni-PS condition was higher; however, the mechanism behind this enhancement remains to be studied. Future studies should compare the performance of using PS and Ni-PS, while analyzing the microbial communities and DIET-related genes to determine the mechanism behind the improved methanogenesis. Furthermore, the optimal amount of sponge to maximize the effect on AD performance was not investigated, and this study was conducted at a low OLR for only 1 month. Therefore, future research should address optimizing the ratio of Ni-PS to sludge and evaluating the performance of Ni-PS in a longer continuous experiment with a higher OLR in the AD system

Acknowledgements

I would like to express my deepest gratitude to my supervisor, Professor Dr. Junichi Ida, for his invaluable guidance, his mentorship and his support throughout my academic growth during this exchange year at Soka University in Tokyo, Japan. I am also profoundly thankful to Professor Dr. Tatsuchi Matsuyama for his insightful recommendations and advice during my research. His expertise greatly enhanced the quality of my work.

Special thanks to Raul Muñoz for his constant support in managing my exchange program with Soka University. His efforts made my experience seamless and productive.

I am immensely grateful to Stella Chan On San for her guidance and assistance in planning experiments, sharing her knowledge, engaging in discussions about experiment results, and helping with the writing of my thesis. Her contributions were vital to my success.

I extend my sincere appreciation to all the members of the Toda laboratory for providing essential materials and for their kind assistance. Their help was crucial in the completion of my research.

I would like to thank the Hikifune company for supplying the solutions needed for the sponge plating, and the Hokubu sludge treatment center for providing experimental materials for this study.

My heartfelt thanks go to Soka University, not only for offering me the opportunity to complete my thesis abroad but also for supporting me financially with a scholarship.

Lastly, I would like to express my deepest gratitude to my parents, Roberto Alvarez and Maria Jesus de la Torre, for their unconditional support throughout my academic

journey, both in Spain and abroad. Their encouragement has been a constant source of strength and inspiration.

References

Abdelsalam, E., Samer, M., Attia, Y., Abdel-Hadi, M., Hassan, H., & Badr, Y. (2016). Comparison of nanoparticles effects on biogas and methane production from anaerobic digestion of cattle dung slurry. *Renewable Energy*, 87, 592–598. https://doi.org/10.1016/j.renene.2015.10.053

Agboola O, Sadiku RE, Biotidara OF (2012) The properties and the efect of operating parameters on nickel plating. *Int J Phys Sci* 7(3):349–360

Angelidaki, I., Ellegaard, L., & Ahring, B. K. (2003). Applications of the anaerobic digestion process. *In Advances in biochemical engineering, biotechnology* (pp. 1–33). https://doi.org/10.1007/3-540-45838-7_1

APHA, 2005. Standard methods for the examination of Water Environment Federation, Washington DC. https://trove.nla.gov.au/work/16646325?qandversionId=38126605.

Baek, G., Kim, J., Kim, J., & Lee, C. (2018). Role and potential of direct interspecies electron transfer in anaerobic digestion. *Energies*, 11(1), 107. https://www.mdpi.com/1996-1073/11/1/107

Bobade, V., & Lomte, A. T. (2015). Challenges in UASB reactor system design: *A Review. ResearchGate.* https://www.researchgate.net/publication/283495427_Challenges_in_UASB_reactor_system_design_A_Review

Boletín Oficial del Estado. (2015). Ley 35/2015, de 22 de septiembre, de reforma del sistema para la valoración de los daños y perjuicios causados a las personas en accidentes de circulación. *BOE*, 219, 80152-80202. https://www.boe.es/boe/dias/2015/09/12/pdfs/BOE-A-2015-9806.pdf

Bouabidi, Z. B., El-Naas, M. H., & Zhang, Z. (2018). Immobilization of microbial cells for the biotreatment of wastewater: A review. *Environmental Chemistry Letters*, 17(1), 241–257. https://doi.org/10.1007/s10311-018-0795-7

Chen, L., Qin, J., Zhao, Q., & Ye, Z. (2022). Treatment of dairy wastewater by immobilized microbial technology using polyurethane foam as carrier. *Bioresource Technology*, *347*, 126430. https://doi.org/10.1016/j.biortech.2021.126430

Feng, L., He, S., Gao, Z., Zhao, W., Jiang, J., Zhao, Q., & Wei, L. (2023). Mechanisms, performance, and the impact on microbial structure of direct interspecies electron transfer for enhancing anaerobic digestion-A review. *Science of the Total Environment*, 862, 160813. https://doi.org/10.1016/j.scitotenv.2022.160813

Feng, X. M., Karlsson, A., Svensson, B. H., & Bertilsson, S. (2010). Impact of trace element addition on biogas production from food industrial waste - linking process to microbial communities. *FEMS Microbiology Ecology/FEMS Microbiology, Ecology*, 74(1), 226–240. https://doi.org/10.1111/j.1574-6941.2010.00932.x

Fernández, N., Montalvo, S., Fernández-Polanco, F., Guerrero, L., Cortés, I., Borja, R., Sánchez, E., & Travieso, L. (2007). Real evidence about zeolite as microorganisms immobilizer in anaerobic fluidized bed reactors. *Process Biochemistry*, *42*(4), 721–728. https://doi.org/10.1016/j.procbio.2006.12.004

Gahlot, P., Aboudi, K., Ahmed, B., Tawfik, A., Khan, A. A., Khursheed, A., & Tyagi, V. K. (2021). Direct interspecies electron transfer (DIET) via conductive materials in anaerobic digestion of organic wastes. *Elsevier eBooks* (pp. 227–252). https://doi.org/10.1016/b978-0-323-85223-4.00024-5

Gezerman, A. O., & Corbacioglu, B. D. (2010). Analysis of the characteristics of Nickel-Plating baths. *International Journal of Chemistry*, 2(2). https://doi.org/10.5539/ijc.v2n2p124

Glass, J. B., & Orphan, V. J. (2012). Trace metal requirements for microbial enzymes involved in the production and consumption of methane and nitrous oxide. *Frontiers in Microbiology*, *3*. https://doi.org/10.3389/fmicb.2012.00061

Guo, Q., Majeed, S., Xu, R., Zhang, K., Kakade, A., Khan, A., Hafeez, F. Y., Mao, C., Liu, P., & Li, X. (2019). Heavy metals interact with the microbial community and affect biogas production in anaerobic digestion: A review. *Journal of Environmental Management*, 240, 266–272. https://doi.org/10.1016/j.jenvman.2019.03.104

Guo, X., Sun, C., Lin, R., Xia, A., Huang, Y., Zhu, X., Show, P., & Murphy, J. D. (2020). Effects of foam nickel supplementation on anaerobic digestion: Direct interspecies electron transfer. *Journal of Hazardous Materials*, 399, 122830. https://doi.org/10.1016/j.jhazmat.2020.122830

Ha, P. T., Lindemann, S. R., Shi, L., Dohnalkova, A. C., Fredrickson, J. K., Madigan, M. T., & Beyenal, H. (2017). Syntrophic anaerobic photosynthesis via direct interspecies electron transfer. *Nature Communications*, 8(1). https://doi.org/10.1038/ncomms13924

Hatakeyama, T., Takagi, K., & Ito, K. (2015). Biodegradation of cyromazine by melamine-degrading bacteria. *Nippon Nōyaku Gakkaishi*, *41*(1), 20–24. https://doi.org/10.1584/jpestics.d15-044

Haytogiu, B., Demirer, G., & Yetis, U. (2001). Effectiveness of anaerobic biomass in adsorbing heavy metals. *Water Science & Technology*, 44(10), 245–252. https://doi.org/10.2166/wst.2001.0632

He, X., Xu, W., Lu, J., Wu, J., Guo, Z., Wei, X., & Wang, C. (2022). Enhanced direct interspecies electron transfer and methane production during anaerobic digestion of fat, oil, and grease by coupling carbon-based conductive materials and exogenous hydrogen. *Bioresource Technology*, 364, 128083. https://doi.org/10.1016/j.biortech.2022.128083 https://trove.nla.gov.au/work/16646325?q&versionId=38126605https://trove.nla.gov.au/work/16646325?qandversionId=38126605.

Hijazi, O., Abdelsalam, E., Samer, M., Amer, B., Yacoub, I., Moselhy, M., Attia, Y., & Bernhardt, H. (2020). Environmental impacts concerning the addition of trace metals in the process of biogas production from anaerobic digestion of slurry. *Journal of Cleaner Production*, *243*, 118593. https://doi.org/10.1016/j.jclepro.2019.118593

Joicy, A., Seo, H., Lee, M., Song, Y., Jeong, Y., & Ahn, Y. (2022). Influence of applied voltage and conductive material in DIET promotion for methane generation. *International Journal of Hydrogen Energy*, 47(18), 10228–10238. https://doi.org/10.1016/j.ijhydene.2022.01.075

Kato, S., Hashimoto, K., & Watanabe, K. (2011). Methanogenesis facilitated by electric syntrophy via (semi)conductive iron-oxide minerals. *Environmental Microbiology*, 14(7), 1646–1654. https://doi.org/10.1111/j.1462-2920.2011.02611.x

Kato, S., Hashimoto, K., & Watanabe, K. (2012). Microbial interspecies electron transfer via electric currents through conductive minerals. *Proceedings of the National Academy of Sciences of the United States of America*, 109(25), 10042–10046. https://doi.org/10.1073/pnas.1117592109

Kaur, M., Sahoo, P., Kumar, M., Sachdeva, S., & Puri, S. (2021). Effect of metal nanoparticles on microbial community shift and syntrophic metabolism during anaerobic digestion of Azolla microphylla. *Journal of Environmental Chemical Engineering*, 9(5), 105841. https://doi.org/10.1016/j.jece.2021.105841

Kim, J., Choi, H., & Lee, C. (2022). Formation and characterization of conductive magnetite-embedded granules in upflow anaerobic sludge blanket reactor treating dairy wastewater. *Bioresource Technology*, 345, 126492. https://doi.org/10.1016/j.biortech.2021.126492

Ko, J. H., Wang, N., Yuan, T., Lü, F., He, P., & Xu, Q. (2018). Effect of nickel-containing activated carbon on food waste anaerobic digestion. *Bioresource Technology*, 266, 516–523. https://doi.org/10.1016/j.biortech.2018.07.015

Kong, T., & Zhang, W. (2023). Enhanced Anaerobic Digestion Using Conductive Materials through Mediation of Direct Microbial Interspecies Electron Transfer: A Review. *Fermentation*, 9(10), 884. https://doi.org/10.3390/fermentation9100884

Kumar, S. S., Ghosh, P., Kataria, N., Kumar, D., Thakur, S., Pathania, D., Kumar, V., Nasrullah, M., & Singh, L. (2021). The role of conductive nanoparticles in anaerobic digestion: Mechanism, current status and future perspectives. *Chemosphere*, 280, 130601. https://doi.org/10.1016/j.chemosphere.2021.130601

Kurita, T., Mogi, T., & Kimura, K. (2016). Influence of different biofilm carriers on the operation and membrane fouling of submerged membrane bioreactors. *Separation and Purification Technology*, *169*, 43–49. https://doi.org/10.1016/j.seppur.2016.05.026

Li, X., Mo, H., Zhou, C., Ci, Y., Wang, J., & Zang, L. (2021). Nickel foam promotes syntrophic metabolism of propionate and butyrate in anaerobic digestion. *ACS Omega*, 6(32), 21033–21042. https://doi.org/10.1021/acsomega.1c02682

Liu, C., Yuan, X., Zeng, G., Li, W., & Li, J. (2008). Prediction of methane yield at optimum pH for anaerobic digestion of organic fraction of municipal solid waste. *Bioresource Technology*, 99(4), 882–888. https://doi.org/10.1016/j.biortech.2007.01.013

Liu, F., Rotaru, A., Shrestha, P. M., Malvankar, N. S., Nevin, K. P., & Lovley, D. R. (2012). Promoting direct interspecies electron transfer with activated carbon. *Energy & Environmental Science*, 5(10), 8982. https://doi.org/10.1039/c2ee22459c

Liu, Y., Wang, P., Gojenko, B., Yu, J., Wei, L., Luo, D., & Xiao, T. (2021). A review of water pollution arising from agriculture and mining activities in Central Asia: Facts, causes and effects. *Environmental Pollution*, 291, 118209. https://doi.org/10.1016/j.envpol.2021.118209

Loto, C. A. (2016). Electroless Nickel Plating – a review. *Silicon*, 8(2), 177–186. https://doi.org/10.1007/s12633-015-9367-7

Lovley, D. R. (2017b). Syntrophy goes electric: direct interspecies electron transfer. *Annual Review of Microbiology*, 71(1), 643–664. https://doi.org/10.1146/annurev-micro-030117-020420

Lovley, D. R., & Walker, D. J. F. (2019). Geobacter protein nanowires. *Frontiers in Microbiology*, 10. https://doi.org/10.3389/fmicb.2019.02078

Malvankar, N. S., & Lovley, D. R. (2014). Microbial nanowires for bioenergy applications. *Current Opinion in Biotechnology*, 27, 88–95. https://doi.org/10.1016/j.copbio.2013.12.003

Mazur, K., Stefańska, A., & Hebda, M. (2018). Analysis of chemical Nickel-Plating process. *Materials Science*, 54(3), 387–394. https://doi.org/10.1007/s11003-018-0196-x

Mei, R., Nobu, M. K., Narihiro, T., Yu, J., Sathyagal, A., Willman, E., & Liu, W. (2018). Novel Geobacter species and diverse methanogens contribute to enhanced methane production in media-added methanogenic reactors. *Water Research*, 147, 403–412. https://doi.org/10.1016/j.watres.2018.10.026

Moestedt, J., Nordell, E., Yekta, S. S., Lundgren, J., Martí, M., Sundberg, C., Ejlertsson, J., Svensson, B., & Björn, A. (2016). Effects of trace element addition on process stability during anaerobic co-digestion of OFMSW and slaughterhouse waste. *Waste Management*, 47, 11–20. https://doi.org/10.1016/j.wasman.2015.03.007

Morita, M., Malvankar, N. S., Franks, A. E., Summers, Z. M., Giloteaux, L., Rotaru, A. E., Rotaru, C., & Lovley, D. R. (2011). Potential for direct interspecies electron transfer in methanogenic wastewater digester aggregates. *MBio*, 2(4). https://doi.org/10.1128/mbio.00159-11

Park, J., Kang, H., Park, K., & Park, H. (2018). Direct interspecies electron transfer via conductive materials: A perspective for anaerobic digestion applications. *Bioresource Technology*, 254, 300–311. https://doi.org/10.1016/j.biortech.2018.01.095

Rajeshwari, K., Balakrishnan, M., Kansal, A., Lata, K., & Kishore, V. (2000). State-of-the-art of anaerobic digestion technology for industrial wastewater treatment. *Renewable & Sustainable Energy Reviews*, 4(2), 135–156. https://doi.org/10.1016/s1364-0321(99)00014-3

Shete, b. s.; Shinkar, n. p. Dairy Industry Wastewater Sources, Characteristics & its Effects on Environment. *International Journal of Current Engineering and Technology*, v. 3. n. 5. p. 1611- 1615, 2013.

Shitu, A., Zhu, S., Qi, W., Tadda, M. A., Liu, D., & Ye, Z. (2020). Performance of novel sponge biocarrier in MBBR treating recirculating aquaculture systems wastewater: Microbial community and kinetic study. *Journal of Environmental Management*, *275*, 111264. https://doi.org/10.1016/j.jenvman.2020.111264

Souza, M. E. (1986). Criteria for the utilization, design and operation of UASB reactors. Water Science & Technology, 18(12), 55–69. https://doi.org/10.2166/wst.1986.0163

Storck, T., Virdis, B., & Batstone, D. J. (2015). Modelling extracellular limitations for mediated versus direct interspecies electron transfer. *The ISME Journal*, 10(3), 621–631. https://doi.org/10.1038/ismej.2015.139

Sure, S., Ackland, M. L., Torriero, A. a. J., Adholeya, A., & Kochar, M. (2016). Microbial nanowires: an electrifying tale. *Microbiology*, 162(12), 2017–2028. https://doi.org/10.1099/mic.0.000382

Tauber, J., Parravicini, V., Svardal, K., & Krampe, J. (2019). Quantifying methane emissions from anaerobic digesters. *Water Science & Technology*, *80*(9), 1654–1661. https://doi.org/10.2166/wst.2019.415

Tawfik, A., Badr, N., Taleb, E., & El-Senousy, W. (2012). Sewage treatment in an up-flow anaerobic sponge reactor followed by moving bed biofilm reactor based on polyurethane carrier material. *Desalination and Water Treatment*, *37*(1–3), 350–358. https://doi.org/10.1080/19443994.2012.661291

Tawfik, A., Badr, N., Taleb, E., & El-Senousy, W. (2012). Sewage treatment in an up-flow anaerobic sponge reactor followed by moving bed biofilm reactor based on

polyurethane carrier material. *Desalination and Water Treatment*, 37(1–3), 350–358. https://doi.org/10.1080/19443994.2012.661291

Tian, Y., Zhang, H., Chai, Y., Wang, L., Mi, X., Zhang, L., & Ware, M. A. (2016). Biogas properties and enzymatic analysis during anaerobic fermentation of Phragmites australis straw and cow dung: influence of nickel chloride supplement. *Biodegradation*, 28(1), 15–25. https://doi.org/10.1007/s10532-016-9774-5

Van Lier, J. B., Vashi, A., Van Der Lubbe, J., & Heffernan, B. (2010). Anaerobic Sewage Treatment using UASB Reactors: Engineering and Operational Aspects. *In IMPERIAL COLLEGE PRESS eBooks* (pp. 59–89). https://doi.org/10.1142/9781848165434_0004

Wang, Z., Wang, T., Si, B., Watson, J., & Zhang, Y. (2021). Accelerating anaerobic digestion for methane production: Potential role of direct interspecies electron transfer. *Renewable & Sustainable Energy Reviews*, 145, 111069. https://doi.org/10.1016/j.rser.2021.111069

Wärff C. (2020). Household wastewater generation model. Report LUTEDX/(TEIE7279)/1-29/(2020), *Division of Industrial Electrical Engineering and Automation*, Lund University, Lund, Sweden.

Wu, Y., Wang, S., Liang, D., & Li, N. (2020). Conductive materials in anaerobic digestion: From mechanism to application. *Bioresource Technology*, 298, 122403. https://doi.org/10.1016/j.biortech.2019.122403

Xiao, L., Lichtfouse, E., & Kumar, P. S. (2021). Advantage of conductive materials on interspecies electron transfer-independent acetoclastic methanogenesis: A critical review. *Fuel*, 305, 121577. https://doi.org/10.1016/j.fuel.2021.121577

Xiao, L., Lichtfouse, E., & Kumar, P. S. (2021). Advantage of conductive materials on interspecies electron transfer-independent acetoclastic methanogenesis: A critical review. *Fuel*, 305, 121577. https://doi.org/10.1016/j.fuel.2021.121577

Xu, S., Sun, M., Thompson, A., & Hu, Z. (2017). Biodegradation and toxicity of melamine at high activated sludge concentrations in a membrane bioreactor. *Water Science & Technology*, *77*(4), 979–987. https://doi.org/10.2166/wst.2017.614

Yan, Y., Zhang, J., Tian, L., Yan, X., Du, L., Leininger, A., Zhang, M., Li, N., Ren, Z. J., & Wang, X. (2023). DIET-like mutualism of Geobacter and methanogens at specific electrode potential boosts production of both methane and hydrogen from propionate. *Water Research*, 235, 119911. https://doi.org/10.1016/j.watres.2023.119911

Yang, L., Huang, Y., Zhao, M., Huang, Z., Miao, H., Xu, Z., & Ruan, W. (2015). Enhancing biogas generation performance from food wastes by high-solids thermophilic anaerobic digestion: Effect of pH adjustment. *International Biodeterioration & Biodegradation*, *105*, 153–159. https://doi.org/10.1016/j.ibiod.2015.09.005

Yang, Y., Tada, C., Miah, M. S., Tsukahara, K., Yagishita, T., & Sawayama, S. (2004). Influence of bed materials on methanogenic characteristics and immobilized microbes in anaerobic digester. *Materials Science & Engineering. C, Biomimetic Materials, Sensors and Systems*, 24(3), 413–419. https://doi.org/10.1016/j.msec.2003.11.005

Zhang, L., Yang, J., Hira, D., Fujii, T., Zhang, W., & Furukawa, K. (2011). High-rate nitrogen removal from anaerobic digester liquor using an up-flow anammox reactor with polyethylene sponge as a biomass carrier. *Journal of Bioscience*

and Bioengineering, *111*(3), 306–311. https://doi.org/10.1016/j.jbiosc.2010.10.010

Zhang, W., Zhang, L., & Li, A. (2015). Enhanced anaerobic digestion of food waste by trace metal elements supplementation and reduced metals dosage by green chelating agent [S, S]-EDDS via improving metals bioavailability. *Water Research*, 84, 266–277. https://doi.org/10.1016/j.watres.2015.07.010

Zhao, B., Zheng, P., Yang, Y., Sha, H., Cao, S., Wang, G., & Zhang, Y. (2022). Enhanced anaerobic digestion under medium temperature conditions: Augmentation effect of magnetic field and composites formed by titanium dioxide on the foamed nickel. *Energy*, 257, 124791. https://doi.org/10.1016/j.energy.2022.124791

Zhao, Z., Zhang, Y., Woodard, T., Nevin, K., & Lovley. (2015). Enhancing syntrophic metabolism in up-flow anaerobic sludge blanket reactors with conductive carbon materials. *Bioresource Technology*, 191, 140–145. https://doi.org/10.1016/j.biortech.2015.05.007

Zhao, Z., Zhang, Y., Yu, Q., Dang, Y., Li, Y., & Quan, X. (2016). Communities stimulated with ethanol to perform direct interspecies electron transfer for syntrophic metabolism of propionate and butyrate. *Water Research*, 102, 475–484. https://doi.org/10.1016/j.watres.2016.07.005

ユケン工業株式会社. (n.d.). YUKEN INDUSTRY CO.,LTD‖Our techinical skill>Basic Knowledge of Surface Treatment：*Resin Plating*. Copyright 2008-2021 by My Website. https://www.yuken-ind.co.jp/en-US/technology/knowledge/knowledge05.html